

# Decay $B_c^+ \rightarrow D_{(s)}^{(*)+} \ell^+ \ell^-$ within covariant confined quark model

M. A. Ivanov,<sup>1,\*</sup> J. N. Pandya,<sup>2,†</sup> P. Santorelli,<sup>3,4,‡</sup> and N. R. Soni<sup>4,§</sup>

<sup>1</sup>*Bogoliubov Laboratory of Theoretical Physics, Joint  
Institute for Nuclear Research, 141980 Dubna, Russia*

<sup>2</sup>*Department of Physics, Sardar Patel University,  
Vallabh Vidyanagar 388120, Gujarat, India.*

<sup>3</sup>*Dipartimento di Fisica “E. Pancini”, Università di Napoli Federico II - Complesso  
Universitario di Monte S. Angelo Edificio 6, via Cintia, 80126 Napoli, Italy*

<sup>4</sup>*INFN sezione di Napoli - Complesso Universitario di  
Monte S. Angelo Edificio 6, via Cintia, 80126 Napoli, Italy*

(Dated: April 24, 2024)

## Abstract

Here we study the rare decay of  $B_c$  mesons within the effective field theoretical framework of covariant confined quark model. The transition form factors corresponding to  $B_c^+ \rightarrow D^{(*)+}$  and  $B_c^+ \rightarrow D_s^{(*)+}$  are computed in the entire  $q^2$  range. Using form factors we compute the branching fractions and compare with the available theoretical approaches. We also compute other physical observables such as forward backward asymmetry, longitudinal and transverse polarizations and various clean angular observables.

---

\* ivanovm@theor.jinr.ru

† jnpandya-phy@spuvvn.edu

‡ pietro.santorelli@na.infn.it

§ nakulphy@gmail.com, nakul.soni@na.infn.it

## I. INTRODUCTION

$B_c$  meson is one of the very interesting meson having both heavy quarks with different flavor and the mass below  $B\bar{D}$  threshold. Sometimes it is also considered to be in the heavy quarkonia sector, however unlike charmonia and bottomonia  $B_c$  meson can decay through the weak interactions only. This can also be justified by the lifetime of  $B_c$  mesons and consequently, it serves as one of the best candidate for the hunt of new physics beyond standard model. Semileptonic decay of  $B$  meson corresponding to the transition  $b \rightarrow c\ell\nu_\ell$  is explored in great depth by experimental facilities world wide and their results are deviating from the standard model predictions [1–7]. LHCb also reported semileptonic decay of  $B_c$  meson and ratio of branching fractions  $R(J/\psi) = \mathcal{B}(B_c \rightarrow J/\psi\tau^+\nu_\tau)/\mathcal{B}(B_c \rightarrow J/\psi\mu^+\nu_\mu) = 0.71 \pm 0.17(\text{stat}) \pm 0.18(\text{syst})$  [8]. Following this observation, HPQCD collaboration performed the computation of observables corresponding to the lepton flavor universality violation from lattice QCD and determined the ratio  $R(J/\psi) = 0.2582(38)$  which is found to be smaller LHCb measurement at  $1.8\sigma$  [9].

However, rare semileptonic decays are yet to be fully explored by the experimental side. In the past, several anomalies have been reported in  $B \rightarrow K^{(*)}\ell\ell$  corresponding to the  $b \rightarrow s\ell\ell$  channel. Several experimental facilities world wide including LHCb, Belle, BaBar have provided information regarding this channels in great detail. Further,  $B_s \rightarrow \phi\ell\ell$  has also been observed by the world wide experimental facilities. The key observations are the ratio  $R_{K^{(*)}} = \mathcal{B}(B \rightarrow K^{(*)}\mu^+\mu^-)/\mathcal{B}(B \rightarrow K^{(*)}e^+e^-)$  and some other observables including forward backward asymmetry, polarization and different angular observables are deviating by  $2 - 3\sigma$  from the standard model predictions [10–21]. These observations essentially lead to the search for the new physics beyond standard model which are discussed in the framework of light cone sum rules [22, 23], effective theories [24–30] and several other theoretical approaches. In recent developments, simultaneous measurements of  $R_K$  and  $R_{K^*}$  in low and central  $q^2$  range corresponding to  $q^2 \in [0.1, 1.1] \text{ GeV}^2/c^4$  and  $q^2 \in [1.1, 6] \text{ GeV}^2/c^4$  shows very good agreement with standard model predictions at  $0.2\sigma$  [31, 32].

In the similar way,  $b \rightarrow d\ell\ell$  can also be a potential mode for the search of new physics. For the transition corresponding to the  $b \rightarrow d$ , LHCb and Belle collaborations have provided some of the important data for the channels  $B \rightarrow (\rho, \omega, \pi, \eta)\ell^+\ell^-$  and  $B_s^0 \rightarrow \bar{K}^{*0}\mu^+\mu^-$  [33–35]. Furthermore, LHCb collaboration has also provided the relative ratios for  $b \rightarrow$

$d/b \rightarrow s$  transition in the channels  $\mathcal{B}(B^+ \rightarrow \pi^+\mu^+\mu^-)/\mathcal{B}(B^+ \rightarrow K^+\mu^+\mu^-)$  and  $\mathcal{B}(B_s^0 \rightarrow \bar{K}^{*0}\mu^+\mu^-)/\mathcal{B}(\bar{B}^0 \rightarrow \bar{K}^{*0}\mu^+\mu^-)$  [36, 37]. Several anomalies regarding these studies are reported in the book [38] and in review article [39] and references therein.

All these anomalies can also be tested in the rare semileptonic decay of  $B_c$  meson where the decay channels  $B_c^+ \rightarrow D^{(*)+}\ell^+\ell^-$  and  $B_c^+ \rightarrow D_s^{(*)+}\ell^+\ell^-$  can also prove to be important candidates for the search towards any new physics beyond standard model. These modes are yet to be identified precisely by the world wide experimental facilities as well as the lattice simulations. The obvious reasons behind this is very less branching fractions making it difficult to probe in presence of background. Also  $B_c$  mesons are produced less frequently with compared to other bottom mesons and that is also the reason why the excited states are not explored well yet. Very recently, LHCb collaboration also set the upper limit for the channel  $B_c^+ \rightarrow D_s^+\mu^+\mu^-$  along with the fragmentation fractions of  $B$  meson with  $c$  and  $u$  quarks at 95% confidence interval [40]. Whereas on theoretical front, semileptonic as well as rare semileptonic decays are explored using various approaches. Geng *et al.*, studied rare semileptonic decays are studied using light front quark model and constituent quark model [41]. Azizi *et al.*, also studied these channels using the three point QCD sum rules [42, 43]. Faessler *et al.*, also studied the exclusive rare decays  $B_c \rightarrow D^{(*)}\ell\ell$  using the relativistic quark model [44]. Choi H. M. studied the transition form factors and different physical observables using the light front quark model [45]. These rare decays are studied using the perturbative QCD approach [46] as well as using the framework of single universal extra dimension [47]. Rare semileptonic decays of  $B$  and  $B_c$  mesons are also studied using the relativistic quark model RQM [48]. The transition form factors computed in relativistic quark model [48] are also employed for study of rare semileptonic decays with non universal  $Z'$  effect [49] as well as using two Higgs doublet model [50]. Further, these form factors are also employed for the search of new physics in different observables [51–53].

In present work, we study the rare semileptonic decay for the channels  $B_c^+ \rightarrow D_{(s)}^{(*)+}\ell^+\ell^-$  for  $\ell = e, \mu, \tau$  and  $\nu$  which are essentially the transitions corresponding to  $b \rightarrow d(s)\ell^+\ell^-$ . The necessary transition form factors are computed in the entire range of momentum transfer squared by employing the covariant confined quark model (CCQM) with built-in infrared confinement and then utilised further for computation of branching fractions. We also compute some more physical observables such as forward backward asymmetry, longitudinal and transverse polarizations and different other angular observables. We also made brief com-

parison of our finding with the available experimental data and theoretical predictions. We further compare our results of different observables with the available theoretical approaches. In the past, we have successfully employed CCQM for predicting various transitions for charm as well as bottom hadrons which shows the ingenuity of the model [54–60].

This paper is organised in the following way: After the brief introduction to the subject with the recent literature reports in sec. I, we introduce theoretical model i.e. covariant confined quark model (CCQM) in sec. II. In this section, we provide the Wilson coefficients and transition form factors and the relations of various observables such as branching fractions, forward backward asymmetry, longitudinal and transverse polarizations, and angular observables. Then in sec. IV, we list all the numerical results along with the comparison with theoretical approaches. Finally we summarise the present work in sec. V.

## II. THEORETICAL FRAMEWORK

Within the standard model (SM), the effective Hamiltonian for the  $b \rightarrow q\ell^+\ell^-$  decay can be written in terms of the following operators [63–65]

$$\mathcal{H}_{eff}^{SM} = -\frac{4G_F}{\sqrt{2}}V_{tq}^*V_{tb} \left\{ \sum_{i=1}^{10} C_i(\mu)\mathcal{O}_i(\mu) + \frac{V_{ub}^*V_{uq}}{V_{tb}^*V_{tq}} \sum_{i=1}^2 C_i(\mu)[\mathcal{O}_i(\mu) - \mathcal{O}_i^u(\mu)] \right\}, \quad (1)$$

where  $q = d$  for  $b \rightarrow d\ell^+\ell^-$  and  $q = s$  for  $b \rightarrow s\ell^+\ell^-$ .

In the above equation,  $C_i$  are the Wilson coefficients and the set of local operators  $\mathcal{O}_i$  obtained within the SM for  $b \rightarrow s\ell^+\ell^-$  as well for  $b \rightarrow d\ell^+\ell^-$  transition using a standard procedure [64, 65]. These operators include current-current operators ( $\mathcal{O}_{1,2}$ ), QCD penguin operators ( $\mathcal{O}_{3-6}$ ), dipole operators ( $\mathcal{O}_{7,8}$ ) and electroweak semileptonic penguin operators

TABLE I. Values of the input parameters [61] and Wilson coefficients [62].

$m_W$	$\sin^2 \theta_W$	$\alpha(M_Z)$	$\bar{m}_c$	$\bar{m}_b$	$\bar{m}_t$			
80.41 GeV	0.2313	1/128.94	1.27 GeV	4.68 GeV	173.3 GeV			
$C_1$	$C_2$	$C_3$	$C_4$	$C_5$	$C_6$	$C_7^{\text{eff}}$	$C_9$	$C_{10}$
-0.2632	1.0111	-0.0055	-0.0806	0.0004	0.0009	-0.2923	4.0749	-4.3085

( $\mathcal{O}_{9,10}$ ). Within SM, these operators  $\mathcal{O}_i$  and  $\mathcal{O}_i^u$  defined as

$$\begin{aligned}
\mathcal{O}_1^u &= (\bar{q}_{a_1} \gamma^\mu P_L u_{a_2})(\bar{u}_{a_2} \gamma_\mu P_L b_{a_1}), & \mathcal{O}_2^u &= (\bar{q} \gamma^\mu P_L u)(\bar{u} \gamma_\mu P_L b), \\
\mathcal{O}_1 &= (\bar{q}_{a_1} \gamma^\mu P_L c_{a_2})(\bar{c}_{a_2} \gamma_\mu P_L b_{a_1}), & \mathcal{O}_2 &= (\bar{q} \gamma^\mu P_L c)(\bar{c} \gamma_\mu P_L b), \\
\mathcal{O}_3 &= (\bar{q} \gamma^\mu P_L b) \sum_{q'} (\bar{q}' \gamma_\mu P_L q'), & \mathcal{O}_4 &= (\bar{q}_{a_1} \gamma^\mu P_L b_{a_2}) \sum_{q'} (\bar{q}'_{a_2} \gamma_\mu P_L q'_{a_1}), \\
\mathcal{O}_5 &= (\bar{q} \gamma^\mu P_L b) \sum_{q'} (\bar{q}' \gamma_\mu P_R q'), & \mathcal{O}_6 &= (\bar{q}_{a_1} \gamma^\mu P_L b_{a_2}) \sum_{q'} (\bar{q}'_{a_2} \gamma_\mu P_R q'_{a_1}), \\
\mathcal{O}_7 &= \frac{e}{16\pi^2} \bar{m}_b (\bar{q} \sigma^{\mu\nu} P_R b) F_{\mu\nu}, & \mathcal{O}_8 &= \frac{g}{16\pi^2} \bar{m}_b (\bar{q}_{a_1} \sigma^{\mu\nu} P_R \mathbf{T}_{a_1 a_2} b_{a_2}) \mathbf{G}_{\mu\nu}, \\
\mathcal{O}_9 &= \frac{e^2}{16\pi^2} (\bar{q} \gamma^\mu P_L b)(\bar{\ell} \gamma_\mu \ell), & \mathcal{O}_{10} &= \frac{e^2}{16\pi^2} (\bar{q} \gamma^\mu P_L b)(\bar{\ell} \gamma_\mu \gamma_5 \ell),
\end{aligned} \tag{2}$$

Here,  $G_{\mu\nu}$  is the gluon field strength,  $F_{\mu\nu}$  is the photon field strength,  $a_{1,2}$  denote the color indices,  $T_{a_1, a_2}$  are the SU(3) color generators,  $P_{L,R}$  are the chirality projection operator and  $\mu$  is the renormalization scale. Matrix element for the channels  $B_c \rightarrow D_{(s)}^{(*)} \ell^+ \ell^-$  can be written as [63, 64]

$$\begin{aligned}
\mathcal{M}(B_c \rightarrow D_{(s)}^{(*)} \ell^+ \ell^-) &= \frac{G_F \alpha}{\sqrt{2} \pi} V_{tq}^* V_{tb} \left\{ C_9^{\text{eff}} \langle D_{(s)}^{(*)} | \bar{q} \gamma_\mu P_L b | B_c \rangle (\bar{\ell} \gamma^\mu \ell) + C_{10} \langle D_{(s)}^{(*)} | \bar{q} \gamma_\mu P_L b | B_c \rangle (\bar{\ell} \gamma^\mu \gamma_5 \ell) \right. \\
&\quad \left. - \frac{2\bar{m}_b}{q^2} C_7^{\text{eff}} \langle D_{(s)}^{(*)} | \bar{q} i \sigma^{\mu\nu} q_\nu P_R b | B_c \rangle (\bar{\ell} \gamma^\mu \ell) \right\}, \tag{3}
\end{aligned}$$

Here  $C_9^{\text{eff}}(\mu)$  contains the corrections to the four-quark operators  $\mathcal{O}_{1-6}$  and  $\mathcal{O}_{1,2}^u$  in Eq. (1) in the form of [66–74]

$$C_9^{\text{eff}}(\mu) = \xi_1 + \lambda_q^* \xi_2, \tag{4}$$

with

$$\begin{aligned}
\xi_1 &= C_9 + C_0 h^{\text{eff}}(\hat{m}_c, \hat{s}) - \frac{1}{2} h(1, \hat{s})(4C_3 + 4C_4 + 3C_5 + C_6) \\
&\quad - \frac{1}{2} h(0, \hat{s})(C_3 + 3C_4) + \frac{2}{9}(3C_3 + C_4 + 3C_5 + C_6) \tag{5}
\end{aligned}$$

$$\xi_2 = \left[ h^{\text{eff}}(\hat{m}_c, \hat{s}) - h^{\text{eff}}(\hat{m}_u, \hat{s}) \right] (3C_1 + C_2) \tag{6}$$

where  $C_0 \equiv 3C_1 + C_2 + 3C_3 + C_4 + 3C_5 + C_6$  and  $\lambda_d = (V_{ub}^* V_{ud}) / (V_{tb}^* V_{td})$  for the transition corresponding to the  $b \rightarrow d \ell^+ \ell^-$  and  $\lambda_s = (V_{ub}^* V_{us}) / (V_{tb}^* V_{ts})$  for the transition corresponding to the  $b \rightarrow s \ell^+ \ell^-$ . Further, the quark-loop contribution is given by

$$h(\hat{m}_q, \hat{s}) = -\frac{8}{9} \ln \hat{m}_q + \frac{8}{27} + \frac{4}{9}x - \frac{2}{9}(2+x)|1-x|^{1/2} \begin{cases} \left( \ln \left| \frac{\sqrt{1-x}+1}{\sqrt{1-x}-1} \right| - i\pi \right), & \text{for } x \equiv \frac{4\hat{m}_q^2}{\hat{s}} < 1, \\ 2 \arctan \frac{1}{\sqrt{x-1}}, & \text{for } x \equiv \frac{4\hat{m}_q^2}{\hat{s}} > 1, \end{cases}$$

and

$$h(0, \hat{s}) = \frac{8}{27} - \frac{4}{9} \ln \hat{s} + \frac{4}{9} i\pi,$$

and the functions,

$$h^{\text{eff}}(\hat{m}_c, \hat{s}) = h(\hat{m}_c, \hat{s}) + \frac{3\pi}{\alpha^2 C_0} \sum_{V=J/\psi, \psi(2S), \dots} \frac{m_V \mathcal{B}(V \rightarrow \ell^+ \ell^-) \Gamma_V}{m_V^2 - q^2 - im_V \Gamma_V}, \quad (7)$$

$$h^{\text{eff}}(\hat{m}_u, \hat{s}) = h(\hat{m}_u, \hat{s}) + \frac{3\pi}{\alpha^2 C_0} \sum_{V=\rho^0, \omega, \phi} \frac{m_V \mathcal{B}(V \rightarrow \ell^+ \ell^-) \Gamma_V}{m_V^2 - q^2 - im_V \Gamma_V} \quad (8)$$

where  $\hat{m}_q = \bar{m}_q/m_1$ ,  $\hat{s} = q^2/m_1^2$  and  $\alpha$  is the coupling constant considered at  $Z$ -boson mass. The nonresonant contribution is computed by ignoring the terms containing the vector resonances in Eq. (7) and (8). The masses, total decay widths and dilepton branching fractions of vector mesons are taken from the PDG book [75]. For the present computations, we consider the next-to-next leading order Wilson coefficients from the Ref. [62] which are essentially evaluated at renormalization scale  $\mu = 2M_W$  and they are computed by renormalization group equation to the hadronic scale  $\mu_b = 4.8$  GeV. The values of input parameters and Wilson coefficients are tabulated in Tab. I.

The transition form factors corresponding to the channels  $B_c^+ \rightarrow D_{(s)}^{(*)+} \ell^+ \ell^-$  are computed in the effective field theoretical framework of CCQM [58, 76–81]. The effective Lagrangian for the interaction between meson and constituent quark can be written in the most common form as

$$\mathcal{L}_{\text{int}} = g_M M(x) \int dx_1 \int dx_2 F_M(x; x_1, x_2) \bar{q}_2(x_2) \Gamma_M q_1(x_1) + \text{H.c.} \quad (9)$$

Here,  $\Gamma_M$  is the Dirac matrix and can take the values according to the type of meson based on the spin.  $F_M$  is the vertex function which describe the effective finite size of the meson given by

$$F_M(x, x_1, x_2) = \delta(x - w_1 x_1 - w_2 x_2) \Phi_M((x_1 - x_2)^2). \quad (10)$$

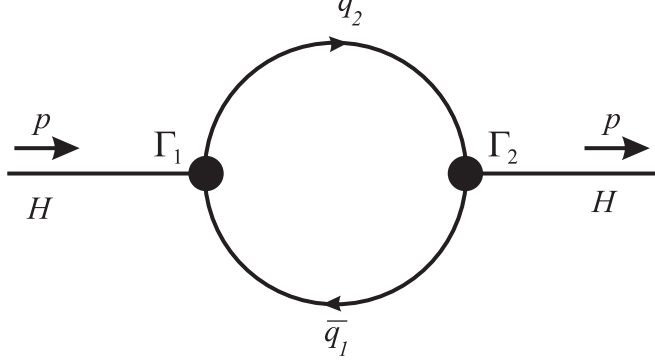


FIG. 1. Feynman diagram for meson mass operator

Here,  $\Phi_M$  is the correlation function for the constituents with masses  $m_{q_{1,2}}$  and mass ratios  $w_i = m_{q_i}/(m_{q_1} + m_{q_2})$ . Next, we consider the vertex function to be of the form of simple Gaussian function with the effective finite size of the meson ( $\Lambda_M$ ). The vertex function takes the form

$$\tilde{\Phi}_M(-k^2) = e^{k^2/\Lambda_M^2} \quad (11)$$

Here, quark masses ( $m_{1,2}$ ) and size parameters ( $\Lambda_M$ ) are the model parameters and are listed in Tab. II. A key feature of choosing the vertex function to have the Gaussian form is that it will make the analytical computation easier.  $g_M$  in Eq. (9) is the coupling constant which characterizes the strength between quarks with the meson. In order to justify the fact that quarks are confined within the hadrons, we use compositeness condition [82, 83] for determination of coupling constants. It is given by setting the renormalization constant ( $Z_M$ ) to be equal to zero as,

$$Z_M = 1 - \frac{3g_M^2}{4\pi^2} \tilde{\Pi}'_M(m_M^2) = 0. \quad (12)$$

Here,  $\tilde{\Pi}_M$  is the meson mass operator given in Fig. 1 defined as

$$\tilde{\Pi}_M(p^2) = N_c g_M^2 \int \frac{d^4k}{(2\pi)^4 i} \tilde{\Phi}_M^2(-k^2) \text{tr}[\Gamma_M S_1(k + w_1 p) \Gamma_M S_2(k - w_2 p)]. \quad (13)$$

Here,  $N_c = 3$  is the number of colours and  $S_{1,2}$  are the free quark propagator which can be written in the form of Fock-Schwinger representation as it provides the additional advantages for the computation of loop integration. All the necessary analytical computation including trace evaluation, loop integration were performed using the FORM language. At the end, a universal infrared parameter  $\lambda = 0.181$  GeV is introduced in order to remove

divergences in the quark loop diagrams. Next, we define the CCQM model parameters such as quark masses ( $m_q$ ) and size parameters  $\Lambda_M$ . In present work, we utilised from the updated least square fit performed in the past CCQM Ref. [58, 84–86]. In these references, the model parameters are determined by fitting the computed observables such as leptonic decay widths, electromagnetic decay widths and meson masses with the experimental data or lattice simulations and the differences are considered to be the absolute uncertainty in the respective size parameter. It is worth noting here that the maximum uncertainty is found to be less than 10% for the computed form factors at the maximum  $q^2$  range. Further, these uncertainties in the form factors are then transported for the branching fraction computations and other physical observables.

With the optimized model parameters and coupling constants, we next compute the transition form factors in the whole  $q^2$  range. The transition form factors for the channels  $B_c^+ \rightarrow D_{(s)}^{(*)+}$  can be written as

$$\begin{aligned}
\langle D_{(s)}(p_2) | \bar{q} O^\mu b | B_c(p_1) \rangle &= N_c g_{B_c} g_{D_{(s)}} \int \frac{d^4 k}{(2\pi)^4 i} \tilde{\phi}_{B_c}(-k + w_{13} p_1)^2 \tilde{\phi}_{D_{(s)}}(-k + w_{23} p_2)^2 \\
&\times \text{tr}[O^\mu S_1(k + p_1) \gamma^5 S_3(k) \gamma^5 S_2(k + p_2)] \\
&= F_+(q^2) P^\mu + F_-(q^2) q^\mu, \\
\langle D_{(s)}(p_2) | \bar{q} \sigma^{\mu\nu} (1 - \gamma^5) b | B_c(p_1) \rangle &= N_c g_{B_c} g_{D_{(s)}} \int \frac{d^4 k}{(2\pi)^4 i} \tilde{\phi}_{B_c}(-k + w_{13} p_1)^2 \tilde{\phi}_{D_{(s)}}(-k + w_{23} p_2)^2 \\
&\times \text{tr}[\sigma^{\mu\nu} (1 - \gamma^5) S_1(k + p_1) \gamma^5 S_3(k) \gamma^5 S_2(k + p_2)] \\
&= \frac{i F_T(q^2)}{m_1 + m_2} (P^\mu q^\nu - P^\nu q^\mu + i \varepsilon^{\mu\nu P q}). \tag{14}
\end{aligned}$$

$$\begin{aligned}
\langle D_{(s)}^*(p_2, \epsilon) | \bar{q} O^\mu b | B_c(p_1) \rangle &= N_c g_{B_c} g_{D_{(s)}^*} \int \frac{d^4 k}{(2\pi)^4 i} \tilde{\phi}_{B_c}(-k + w_{13} p_1)^2 \tilde{\phi}_{D_{(s)}^*}(-k + w_{23} p_2)^2 \\
&\times \text{tr}[O^\mu S_1(k + p_1) \gamma^5 S_3(k) \not{\epsilon}_\nu^\dagger S_2(k + p_2)] \\
&= \frac{\epsilon_\nu^\dagger}{m_1 + m_2} [-g^{\mu\nu} P \cdot q A_0(q^2) + P^\mu P^\nu A_+(q^2) + q^\mu P^\nu A_-(q^2) \\
&+ i \varepsilon^{\mu\nu\alpha\beta} P_\alpha q_\beta V(q^2)], \\
\langle D_{(s)}^*(p_2, \epsilon) | \bar{q} \sigma^{\mu\nu} q_\nu (1 + \gamma^5) b | B_c(p_1) \rangle &= N_c g_{B_c} g_{D_{(s)}^*} \int \frac{d^4 k}{(2\pi)^4 i} \tilde{\phi}_{B_c}(-k + w_{13} p_1)^2 \tilde{\phi}_{D_{(s)}^*}(-k + w_{23} p_2)^2 \\
&\times \text{tr}[\sigma^{\mu\nu} q_\nu (1 + \gamma^5) S_1(k + p_1) \gamma^5 S_3(k) \not{\epsilon}_\nu^\dagger S_2(k + p_2)] \\
&= \epsilon_\nu^\dagger [-(g^{\mu\nu} - q^\mu q^\nu / q^2) P \cdot q a_0(q^2) + i \varepsilon^{\mu\nu\alpha\beta} P_\alpha q_\beta g(q^2) \\
&+ (P^\mu P^\nu - q^\mu P^\nu P \cdot q / q^2) a_+(q^2)]. \tag{15}
\end{aligned}$$

Here, in the above equations,  $P$  is the total momentum of the parent and daughter mesons



and  $q$  is the momentum transfer between parent and daughter mesons. Polarization vector of the daughter meson is defined in such a way that  $\epsilon_\nu^\dagger \cdot p_2 = 0$ .  $p_1^2 = m_{B_c}^2$ ,  $p_2^2 = m_{D(s)^*}^2$ . With all the necessary inputs, the form factors are computed by solving the multidimensional integral using Mathematica in the entire range of momentum transfer squared. We plot the form factors in Eq. (14) and (15) in Fig. 2 and also represented in the double pole approximation as

$$F(q^2) = \frac{F(0)}{1 - a \left( \frac{q^2}{m_1^2} \right) + b \left( \frac{q^2}{m_1^2} \right)^2} \quad (16)$$

The form factors at the maximum recoil  $F(0)$  and double pole parameters  $a$  and  $b$  are listed in Tab. III.

TABLE II. Quark masses, meson size parameters and infra-red cut-off parameter (all in GeV)

$\Lambda_{B_c}$	$\Lambda_D$	$\Lambda_{D^*}$	$\Lambda_{D_s}$	$\Lambda_{D_s^*}$
2.728	1.600	1.529	1.748	1.556
$m_{u/d}$	$m_s$	$m_c$	$m_b$	$\lambda$
0.241	0.428	1.67	5.05	0.181

### III. BRANCHING FRACTIONS AND OTHER PHYSICAL OBSERVABLES

Having determined form factors and Wilson coefficients, we compute the differential decay rates for rare semileptonic decays using the relation [44]

$$\frac{d\Gamma(B_c \rightarrow D(s)^* \ell^+ \ell^-)}{dq^2} = \frac{G_F^2}{(2\pi)^3} \left( \frac{\alpha V_{tb}^* V_{tq}}{2\pi} \right)^2 \frac{|\mathbf{p}_2| q^2 \beta_\ell}{12m_1^2} \mathcal{H}_{\text{tot}}. \quad (17)$$

In the above relation  $\beta_\ell = \sqrt{1 - 4m_\ell^2/q^2}$  and  $|\mathbf{p}_2| = \lambda^{1/2}(m_1^2, m_2^2, q^2)/(2m_1)$  is the momentum of the daughter meson in the rest frame of  $B_c$  meson with  $\lambda(x, y, z)$  to be the Källén function. Further  $m_1 = m_{B_c}$  and  $m_2 = m_{D(s)^*}$ .  $\mathcal{H}_{\text{tot}}$  is the amplitude given here in terms of the helicity amplitudes:

$$\begin{aligned} \mathcal{H}_{\text{tot}} = & \frac{1}{2}(\mathcal{H}_U^{11} + \mathcal{H}_U^{22} + \mathcal{H}_L^{11} + \mathcal{H}_L^{22}) \\ & + \left( \frac{2m_\ell^2}{q^2} \right) \left( \frac{1}{2}\mathcal{H}_U^{11} - \mathcal{H}_U^{22} + \frac{1}{2}\mathcal{H}_L^{11} - \mathcal{H}_L^{22} + \frac{3}{2}\mathcal{H}_S^{22} \right). \end{aligned} \quad (18)$$

TABLE III. Form factors and double pole parameters appeared in Eq. (16)

$F$	$F(0)$	$a$	$b$	$F$	$F(0)$	$a$	$b$
$F_+^{B_c \rightarrow D}$	$0.186 \pm 0.009$	2.352	1.431	$F_-^{B_c \rightarrow D}$	$-0.160 \pm 0.008$	2.424	1.521
$F_T^{B_c \rightarrow D}$	$0.273 \pm 0.013$	2.289	1.326	$F_0^{B_c \rightarrow D}$	$0.186 \pm 0.009$	1.482	0.440
$A_0^{B_c \rightarrow D^*}$	$0.277 \pm 0.006$	1.456	0.181	$A_+^{B_c \rightarrow D^*}$	$0.151 \pm 0.003$	2.161	1.095
$A_-^{B_c \rightarrow D^*}$	$-0.236 \pm 0.005$	2.415	1.465	$V^{B_c \rightarrow D^*}$	$0.231 \pm 0.005$	2.397	1.427
$a_0^{B_c \rightarrow D^*}$	$0.143 \pm 0.003$	1.541	0.304	$a_+^{B_c \rightarrow D^*}$	$0.143 \pm 0.003$	2.153	1.097
$g^{B_c \rightarrow D^*}$	$0.143 \pm 0.003$	2.478	1.561				
$F_+^{B_c \rightarrow D_s}$	$0.255 \pm 0.015$	2.212	1.265	$F_-^{B_c \rightarrow D_s}$	$-0.202 \pm 0.013$	2.271	1.331
$F_T^{B_c \rightarrow D_s}$	$0.362 \pm 0.021$	2.158	1.174	$F_0^{B_c \rightarrow D_s}$	$0.255 \pm 0.015$	1.376	0.326
$A_0^{B_c \rightarrow D_s^*}$	$0.366 \pm 0.010$	1.452	0.189	$A_+^{B_c \rightarrow D_s^*}$	$0.190 \pm 0.005$	2.121	1.055
$A_-^{B_c \rightarrow D_s^*}$	$-0.293 \pm 0.009$	2.353	1.395	$V^{B_c \rightarrow D_s^*}$	$0.282 \pm 0.008$	2.332	1.354
$a_0^{B_c \rightarrow D_s^*}$	$0.180 \pm 0.005$	1.535	0.305	$a_+^{B_c \rightarrow D_s^*}$	$0.180 \pm 0.005$	2.117	1.064
$g^{B_c \rightarrow D_s^*}$	$0.180 \pm 0.005$	2.404	1.472				

The helicity amplitudes here are presented in terms of helicity form factors via the relations for the channels  $B_c \rightarrow D_{(s)}$  as [44, 56]

$$\mathcal{H}_U^{ii} = 0, \quad \mathcal{H}_L^{ii} = |H_0^i|^2, \quad \mathcal{H}_S^{ii} = |H_{t0}^i|^2. \quad (19)$$

with  $i = 1, 2$  and these helicity form factors are related to the invariant form factors via relation

$$\begin{aligned} H_0^i &= \frac{2m_1 |\mathbf{p}_2|}{\sqrt{q^2}} \mathcal{F}_+^i, \\ H_{t0}^i &= \frac{1}{\sqrt{q^2}} ((m_1^2 - m_2^2) \mathcal{F}_+^i + q^2 \mathcal{F}_-^i) \end{aligned} \quad (20)$$

and the invariant form factors  $\mathcal{F}_{+-}^i$  for  $i = 1, 2$  are related to the form factors in Eq. (14) as

$$\begin{aligned} \mathcal{F}_+^1 &= C_9^{\text{eff}} F_+ + C_7^{\text{eff}} F_T \frac{2\bar{m}_b}{m_1 + m_2}, \\ \mathcal{F}_-^1 &= C_9^{\text{eff}} F_- - C_7^{\text{eff}} F_T \frac{2\bar{m}_b}{m_1 + m_2} \frac{m_1^2 - m_2^2}{q^2}, \\ \mathcal{F}_+^2 &= C_{10} F_+ \quad , \quad \mathcal{F}_-^2 = C_{10} F_- . \end{aligned} \quad (21)$$

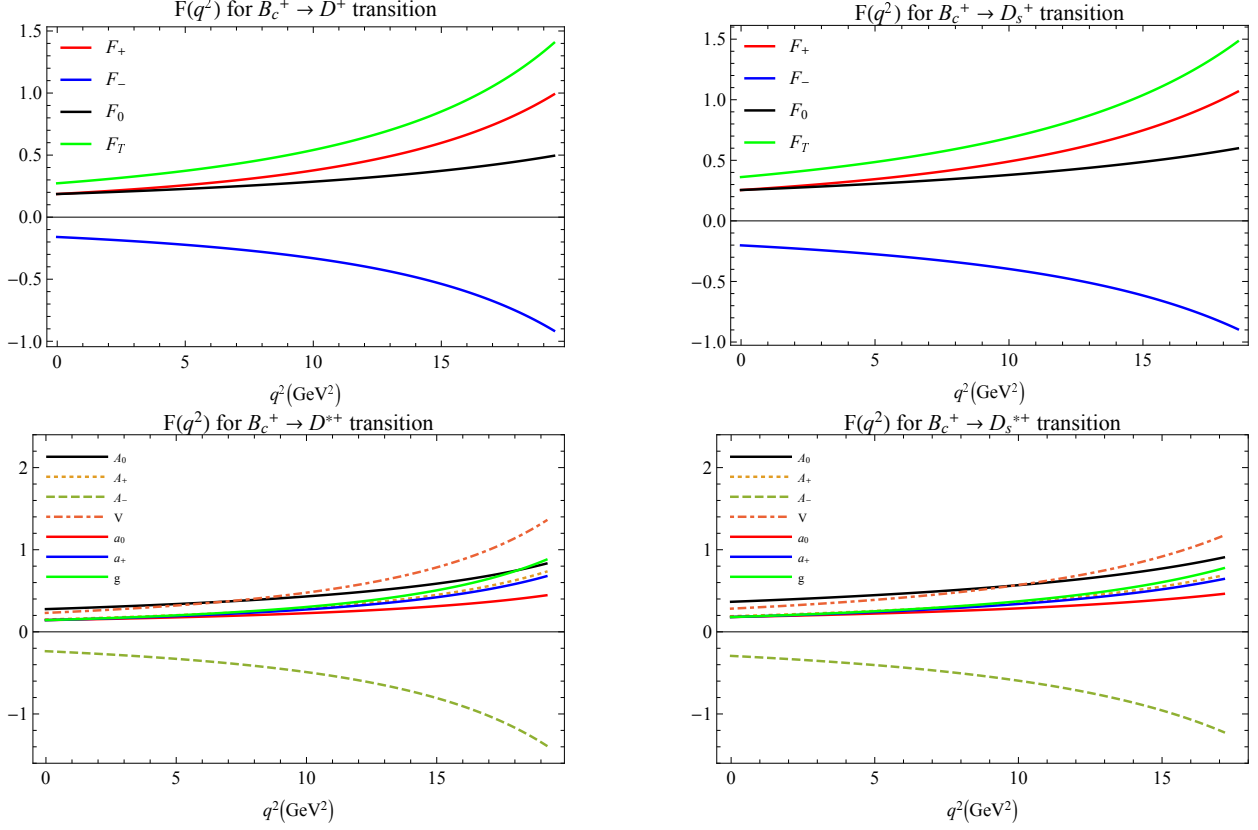


FIG. 2. Form factors

Similarly, helicity amplitudes are presented in terms of helicity form factors via the relations for the channels  $B_c \rightarrow D_{(s)}^*$  as [44, 56]

$$\begin{aligned}\mathcal{H}_U^{ii} &= |H_{+1+1}^i|^2 + |H_{-1-1}^i|^2, \\ \mathcal{H}_L^{ii} &= |H_{00}^i|^2, \quad \mathcal{H}_S^{ii} = |H_{t0}^i|^2,\end{aligned}\tag{22}$$

and these helicity form factors are related to the invariant form factors via relations

$$\begin{aligned}H_{t0}^i &= \frac{1}{m_1 + m_2} \frac{m_1 |\mathbf{p}_2|}{m_2 \sqrt{q^2}} (Pq (-A_0^i + A_+^i) + q^2 A_-^i), \\ H_{\pm 1 \pm 1}^i &= \frac{1}{m_1 + m_2} (-Pq A_0^i \pm 2 m_1 |\mathbf{p}_2| V^i), \\ H_{00}^i &= \frac{1}{m_1 + m_2} \frac{1}{2 m_2 \sqrt{q^2}} \\ &\times (-Pq (m_1^2 - m_2^2 - q^2) A_0^i + 4 m_1^2 |\mathbf{p}_2|^2 A_+^i).\end{aligned}\tag{23}$$

and the invariant form factors  $A^i$  and  $V^i$  ( $i = 1, 2$ ) are related to the form factors in Eq. (15) as

$$\begin{aligned}
V^{(1)} &= C_9^{\text{eff}} V + C_7^{\text{eff}} g \frac{2\bar{m}_b(m_1 + m_2)}{q^2}, \\
A_0^{(1)} &= C_9^{\text{eff}} A_0 + C_7^{\text{eff}} a_0 \frac{2\bar{m}_b(m_1 + m_2)}{q^2}, \\
A_+^{(1)} &= C_9^{\text{eff}} A_+ + C_7^{\text{eff}} a_+ \frac{2\bar{m}_b(m_1 + m_2)}{q^2}, \\
A_-^{(1)} &= C_9^{\text{eff}} A_- + C_7^{\text{eff}} (a_0 - a_+) \frac{2\bar{m}_b(m_1 + m_2)}{q^2} \frac{Pq}{q^2}, \\
V^{(2)} &= C_{10} V, \quad A_0^{(2)} = C_{10} A_0, \quad A_{\pm}^{(2)} = C_{10} A_{\pm}.
\end{aligned} \tag{24}$$

Using the above relations, we plot the differential branching fractions Eq. (17) in Fig. 6 while the computed branching fractions are listed in Tab. IV. We also compare our findings with the results of other theoretical approaches. We also compute branching fractions corresponding to the dimuon channels.

The differential decay width for the transition  $B_c \rightarrow D_{(s)}^{(*)} \nu \bar{\nu}$  can be written as [44, 56]

$$\frac{d\Gamma(B_c^+ \rightarrow D_{(s)}^{(*)+} \nu \bar{\nu})}{dq^2} = \frac{G_F^2}{(2\pi)^3} \left( \frac{\alpha V_{tb}^* V_{tq}}{2\pi} \right)^2 \left[ \frac{D_\nu(x_t)}{\sin^2 \theta_W} \right]^2 \frac{|\mathbf{p}_2| q^2}{4m_1^2} (H_U + H_L), \tag{25}$$

where  $x_t = m_t^2/m_W^2$  and the function  $D_\nu(x_t)$  can be written up to NLO correction as [87–90]

$$D_\nu(x) = D_0(x) + \frac{\alpha_s}{4\pi} D_1(x) \tag{26}$$

with

$$D_0(x) = \frac{x}{8} \left( \frac{2+x}{x-1} + \frac{3x-6}{(x-1)^2} \ln x \right) \tag{27}$$

$$\begin{aligned}
D_1(x) &= -\frac{29x - x^2 - 4x^3}{3(1-x)^2} - \frac{x + 9x^2 - x^3 - x^4}{(1-x)^3} \ln x \\
&+ \frac{8x + 4x^2 + x^3 - x^4}{2(1-x)^3} \ln^2 x - \frac{4x - x^3}{(1-x)^2} \int_1^x dt \frac{\ln t}{1-t} \\
&+ 8x \frac{\partial D_0(x)}{\partial x} \ln \left( \frac{\mu_b^2}{m_W^2} \right).
\end{aligned} \tag{28}$$

As in the previous case, the helicity amplitudes are related to helicity form factors for the channels  $B_c^+ \rightarrow D_{(s)}^+ \nu \bar{\nu}$  as [44, 56]

$$\mathcal{H}_L = |H_0|^2, \quad \mathcal{H}_U = 0 \tag{29}$$

with

$$H_0 = \frac{2m_1 |\mathbf{p}_2|}{\sqrt{q^2}} F_+. \quad (30)$$

instead for the channels  $B_c^+ \rightarrow D_{(s)}^{*+} \nu \bar{\nu}$  as [44, 56]

$$\mathcal{H}_U = |H_{+1+1}|^2 + |H_{-1-1}|^2, \quad \mathcal{H}_L = |H_{00}|^2, \quad (31)$$

with

$$\begin{aligned} H_{\pm 1 \pm 1} &= \frac{1}{m_1 + m_2} (-Pq A_0 \pm 2m_1 |\mathbf{p}_2| V), \\ H_{00} &= \frac{1}{m_1 + m_2} \frac{1}{2m_2 \sqrt{q^2}} (-Pq (m_1^2 - m_2^2 - q^2) A_0 + 4m_1^2 |\mathbf{p}_2|^2 A_+). \end{aligned} \quad (32)$$

The numerical results on the branching fractions are listed in Tab. IV along with the comparison with the results of other theoretical approaches.

We further compute other physical observables such as forward backward asymmetry, longitudinal and transverse polarizations and other clean observables. These lepton flavoured dependent angular observables are related with the helicity amplitudes and to the form factors. Experimental measurements of these observables have played critical role in searching for the physics beyond the standard model for the transition  $b \rightarrow s \ell \ell$  corresponding to the channel  $B \rightarrow K^* \ell \ell$  by LHCb [15, 92] and Bell collaborations [93]. Angular analysis are also observed for the channel  $B_s \rightarrow \phi \mu^+ \mu^-$  and  $\Lambda_b^0 \rightarrow \Lambda \mu^+ \mu^-$  by LHCb collaboration [94, 95]. However, in the other channels, these observables are yet to be identified. Many of these experimental measurements are deviating from the SM predictions and explained using new physics scenario [96–102]. Similar is the case expected corresponding to the  $b \rightarrow d \ell \ell$  transitions. These observables could be helpful in studying the effects of CP violations. Very recently in Ref. [91], these angular observables are computed using the covariant light front quark model in which the transition form factors are obtained using modified Godfrey-Isgur model for the channel  $B_c \rightarrow D_s^* \ell \ell$ . The same observables are also studied for the channels  $\bar{B}_s \rightarrow K^* \ell \ell$  and  $\bar{B} \rightarrow \rho \ell \ell$  using light cone sum rule approach [103]. Recently, some of us have studied these observables in the  $b \rightarrow d \ell^+ \ell^-$  [56] transition. These observables are described in terms of four fold angular distribution and expressed explicitly in terms of helicity form factors. The detailed description and computation techniques of these observables can be found in the Ref. [104, 105]. Relation for these observables reads:

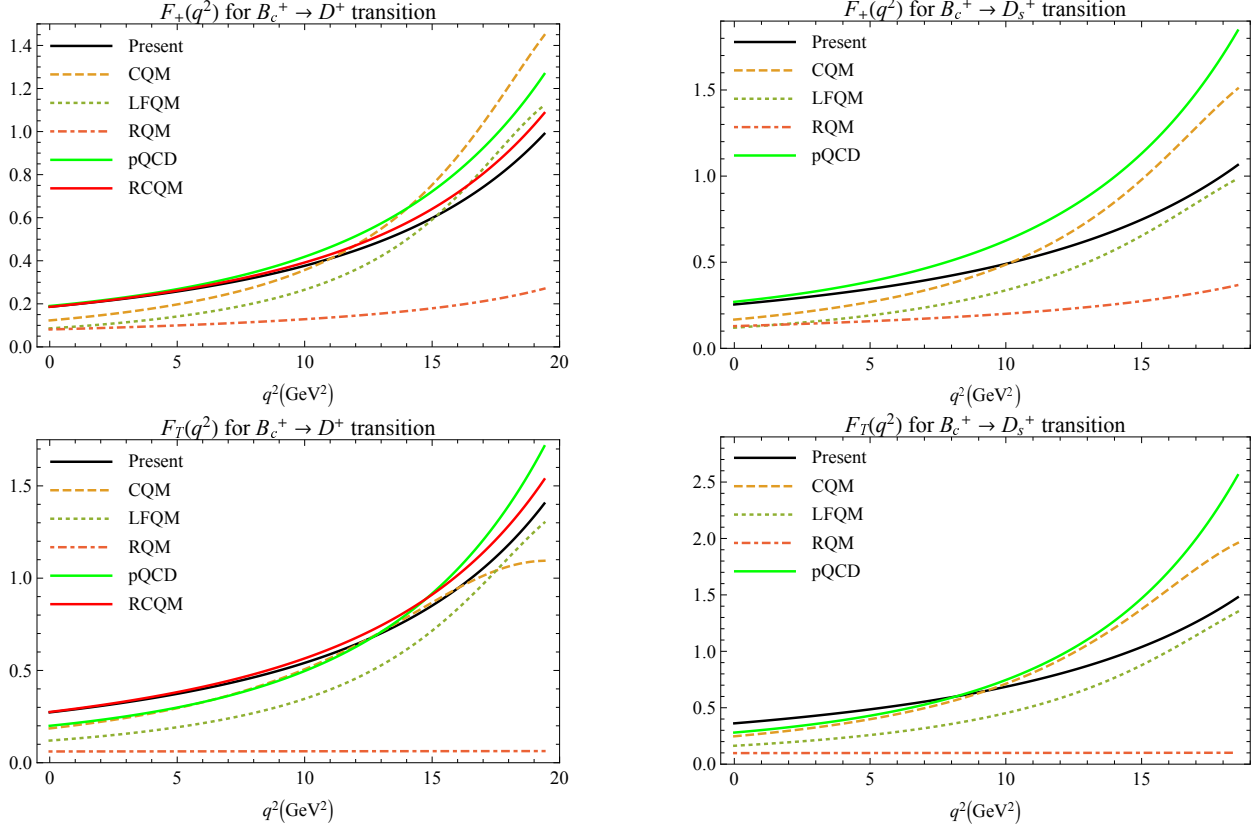


FIG. 3. Form factor comparison for  $B_c \rightarrow D$  (left) and  $B_c \rightarrow D_s$  (right) in comparison with relativistic constituent quark model [44], constituent quark model [41], light front quark model [45], relativistic quark model [48] and perturbative QCD [46].

### 1. Forward backward asymmetry

$$A_{\text{FB}} = \frac{1}{d\Gamma/dq^2} \left[ \int_0^1 - \int_{-1}^0 \right] d\cos\theta \frac{d^2\Gamma}{dq^2 d\cos\theta} = -\frac{3}{4}\beta_\ell \frac{\mathcal{H}_P^{12}}{\mathcal{H}_{\text{tot}}}, \quad (33)$$

### 2. Longitudinal and Transverse polarization fractions

$$F_L = \frac{1}{2}\beta_\ell^2 \frac{\mathcal{H}_L^{11} + \mathcal{H}_L^{22}}{\mathcal{H}_{\text{tot}}}, \quad F_T = \frac{1}{2}\beta_\ell^2 \frac{\mathcal{H}_U^{11} + \mathcal{H}_U^{22}}{\mathcal{H}_{\text{tot}}}, \quad (34)$$

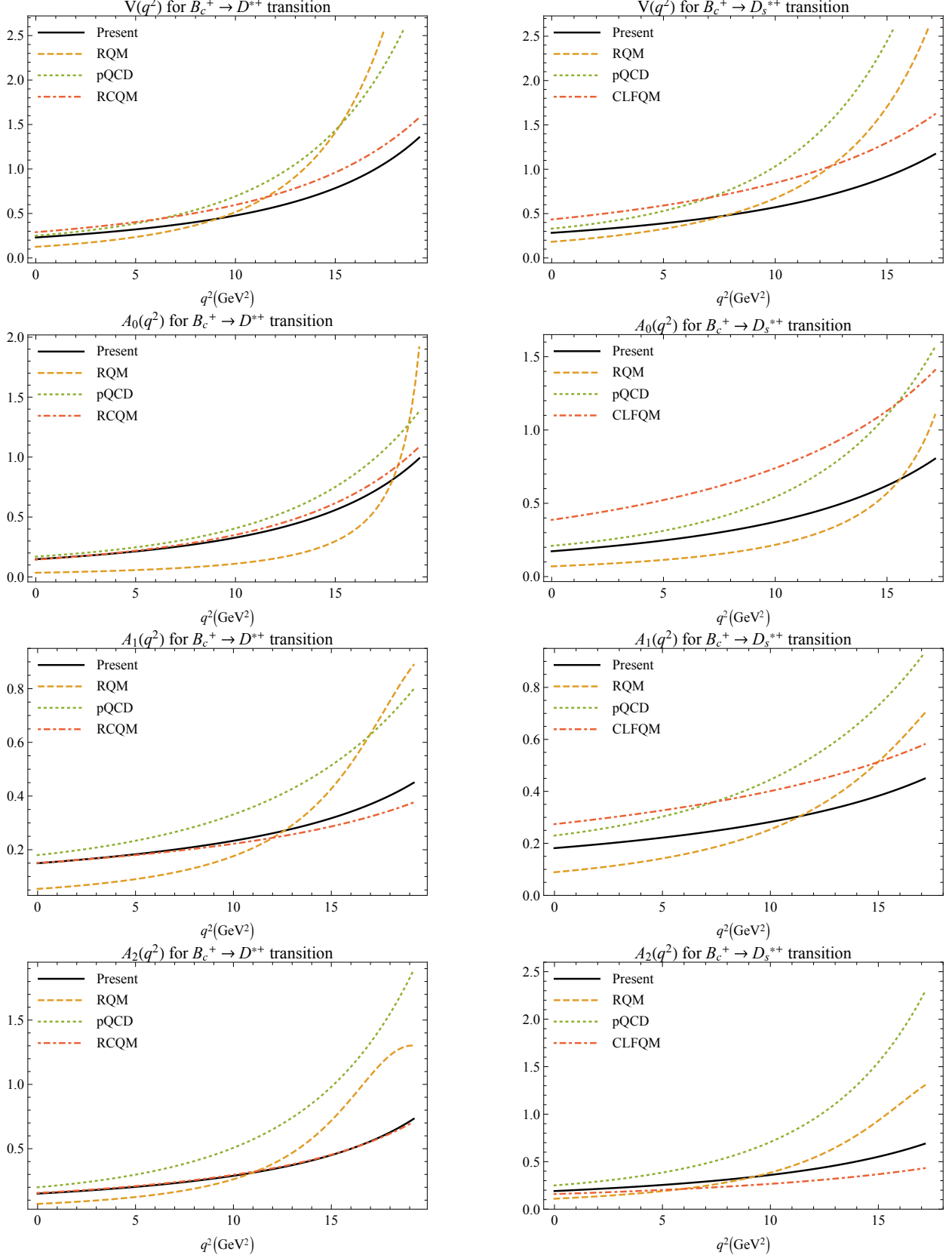


FIG. 4. Form factor comparison for  $B_c \rightarrow D^*$  (left) and  $B_c \rightarrow D_s^*$  (right) in comparison with relativistic constituent quark model [44], relativistic quark model [48], perturbative QCD [46] and covariant light front quark model [91].

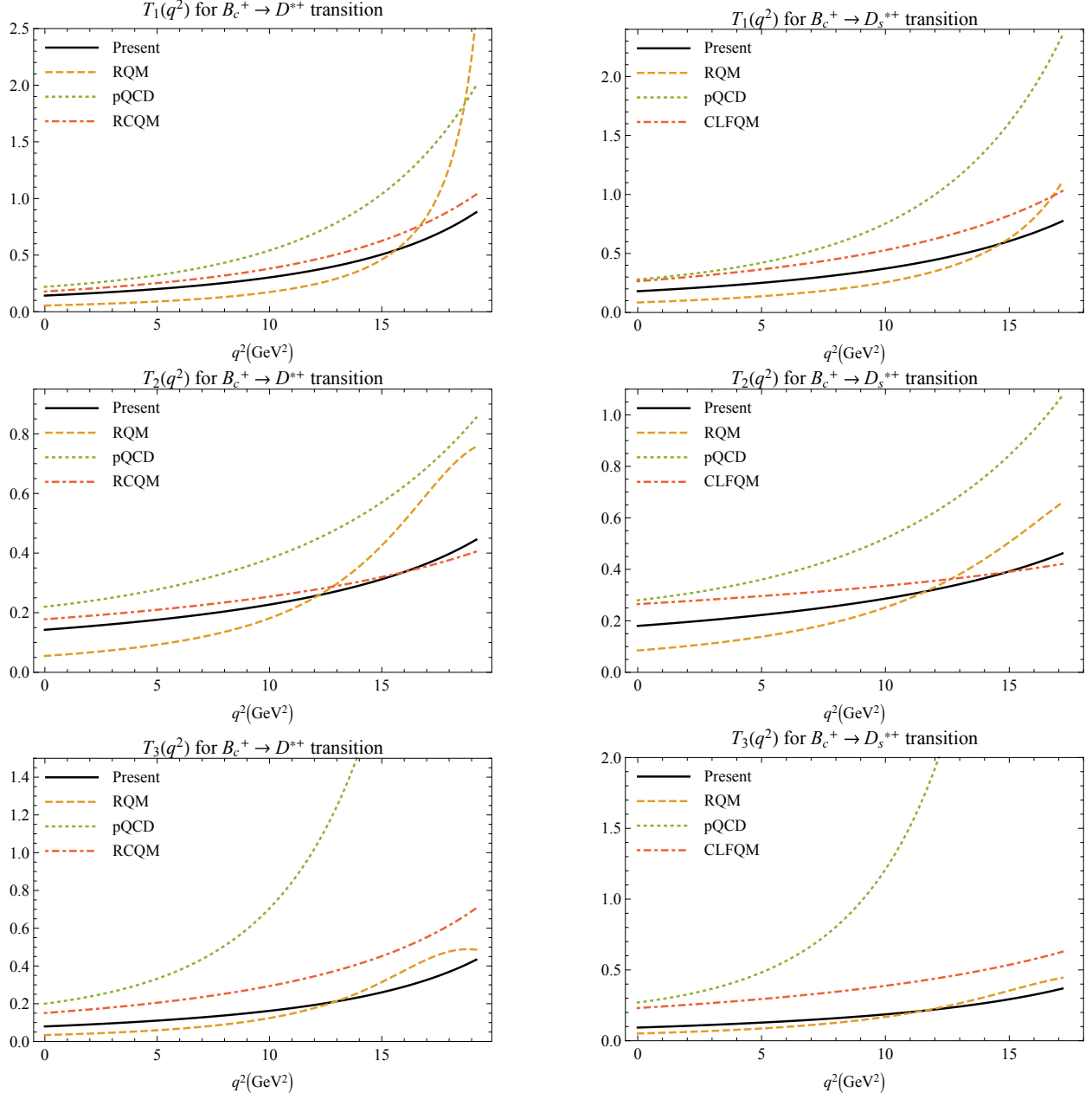


FIG. 5. Same as Fig. 4



### 3. Clean Observables

$$\begin{aligned}
\langle P_1 \rangle_{\text{bin}} &= -2 \frac{\int_{\text{bin}} dq^2 \beta_\ell^2 [\mathcal{H}_T^{11} + \mathcal{H}_T^{22}]}{\int_{\text{bin}} dq^2 \beta_\ell^2 [\mathcal{H}_U^{11} + \mathcal{H}_U^{22}]}, \\
\langle P_2 \rangle_{\text{bin}} &= -\frac{\int_{\text{bin}} dq^2 \beta_\ell \mathcal{H}_P^{12}}{\int_{\text{bin}} dq^2 \beta_\ell^2 [\mathcal{H}_U^{11} + \mathcal{H}_U^{22}]}, \\
\langle P_3 \rangle_{\text{bin}} &= -\frac{\int_{\text{bin}} dq^2 \beta_\ell^2 [\mathcal{H}_{IT}^{11} + \mathcal{H}_{IT}^{22}]}{\int_{\text{bin}} dq^2 \beta_\ell^2 [\mathcal{H}_U^{11} + \mathcal{H}_U^{22}]}, \\
\langle P_4' \rangle_{\text{bin}} &= 2 \frac{\int_{\text{bin}} dq^2 \beta_\ell^2 [\mathcal{H}_I^{11} + \mathcal{H}_I^{22}]}{N_{\text{bin}}}, \\
\langle P_5' \rangle_{\text{bin}} &= -2 \frac{\int_{\text{bin}} dq^2 \beta_\ell [\mathcal{H}_A^{12} + \mathcal{H}_A^{21}]}{N_{\text{bin}}}, \\
\langle P_6' \rangle_{\text{bin}} &= -2 \frac{\int_{\text{bin}} dq^2 \beta_\ell [\mathcal{H}_{II}^{12} + \mathcal{H}_{II}^{21}]}{N_{\text{bin}}}, \\
\langle P_8' \rangle_{\text{bin}} &= 2 \frac{\int_{\text{bin}} dq^2 \beta_\ell^2 [\mathcal{H}_{IA}^{11} + \mathcal{H}_{IA}^{22}]}{N_{\text{bin}}}, \tag{35}
\end{aligned}$$

with the normalization factor  $N_{\text{bin}}$  defined as

$$\mathcal{N}_{\text{bin}} = \sqrt{\int_{\text{bin}} dq^2 \beta_\ell^2 [\mathcal{H}_U^{11} + \mathcal{H}_U^{22}] \cdot \int_{\text{bin}} dq^2 \beta_\ell^2 [\mathcal{H}_L^{11} + \mathcal{H}_L^{22}]}. \tag{36}$$

For computation of expectation value of these observables over bins, we need to multiply by the phase space factor  $|\mathbf{p}_2|q^2\beta_\ell$  in the numerator and denominator separately. The angle appearing in the relation of forward backward asymmetry is the polar angle between the momentum of parent meson and the momentum transfer. Further, bins are corresponding to the momentum transferred square ranges [1.1, 6.0], [6.0, 8.0], [11.0, 12.5] and [15.0, 17.0] GeV<sup>2</sup>.

## IV. RESULTS AND DISCUSSION

Using covariant confined quark model, we compute the transition form factors using the model parameters in Tab. II and we plot them in terms of  $q^2$  in Fig. 2. We also made a comparison of our form factors with the results of various other theoretical prediction such as relativistic constituent quark model (RQM) [44], constituent quark model (CQM) [41], QCD sum rules (QCDSR) [43], light front quark model (LFQM) [45], relativistic quark model (RQM) [48], perturbative QCD (pQCD) [46]. However in order to have the comparison we need to transform our form factors Eq. (14) and (15) with those using BSW form factors

[106]. The transformed form factors are denoted by the primed form factors.

$$F'_0 = F_+ + \frac{q^2}{m_1^2 - m_2^2} F_-, \quad (37)$$

$$A_0 = \frac{m_1 + m_2}{m_1 - m_2} A'_1, \quad A_+ = A'_2,$$

$$A_- = \frac{2m_2(m_1 + m_2)}{q^2} (A'_3 - A'_0), \quad V = V',$$

$$a_0 = T'_2, \quad g = T'_1, \quad a_+ = T'_2 + \frac{q^2}{m_1^2 - m_2^2} T'_3. \quad (38)$$

These form factors also satisfy the constraints

$$\begin{aligned} A'_0(0) &= A'_3(0) \\ 2m_2 A'_3(q^2) &= (m_1 + m_2) A'_1(q^2) - (m_1 - m_2) A'_2(q^2). \end{aligned} \quad (39)$$

For the subsequent section, we remove the prime from the form factors in order to avoid confusion. The graphical comparison between the results can be found in Fig. 3 - 5. It is observed that our results of the form factors for the transition  $B_c \rightarrow D$  are very similar to the pQCD, LFQM, CQM and RCQM predictions. Whereas in comparison with RQM, our results are significantly higher in almost entire  $q^2$  range. For  $B_c \rightarrow D_s$  transition also, our results are in good agreement with the LFQM and CQM predictions. Similarly for  $B_c \rightarrow D_{(s)}^*$  transitions, our form factors are compatible with the RQM and pQCD predictions for the range  $q^2 \rightarrow q_{\text{max}}^2$ , whereas our results are substantially lower for small  $q^2$ . The differences in the predictions are mainly attributed to the different methodology employed for the computation of the transition form factors. Using numerical form factors, we have computed branching fractions of rare semileptonic decays using Eq. (17) and in Fig. 6, we plot differential branching fractions. In Tab. IV, we provide the branching fractions by integrating area under the differential branching fraction curve in Fig. 6. In the differential branching fraction plots, the peaks near to  $q^2 = m_{J/\psi}^2$  and  $q^2 = m_{\psi(2S)}^2$  correspond to the charm resonances and in the low  $q^2$  range in the case of  $B_c \rightarrow D^{(*)}$  transition correspond to the light vector resonances appearing in the effective Wilson coefficients. In Tab. IV, we provide our results considering both resonance as well as non resonance contributions. It is important to note here that in computations of branching fractions, we exclude the experimentally vetoed  $q^2$  range corresponding to the charm resonances. If we include these range, our results are enhanced by an order of magnitude or more. This is also observed in our recent studies [56]

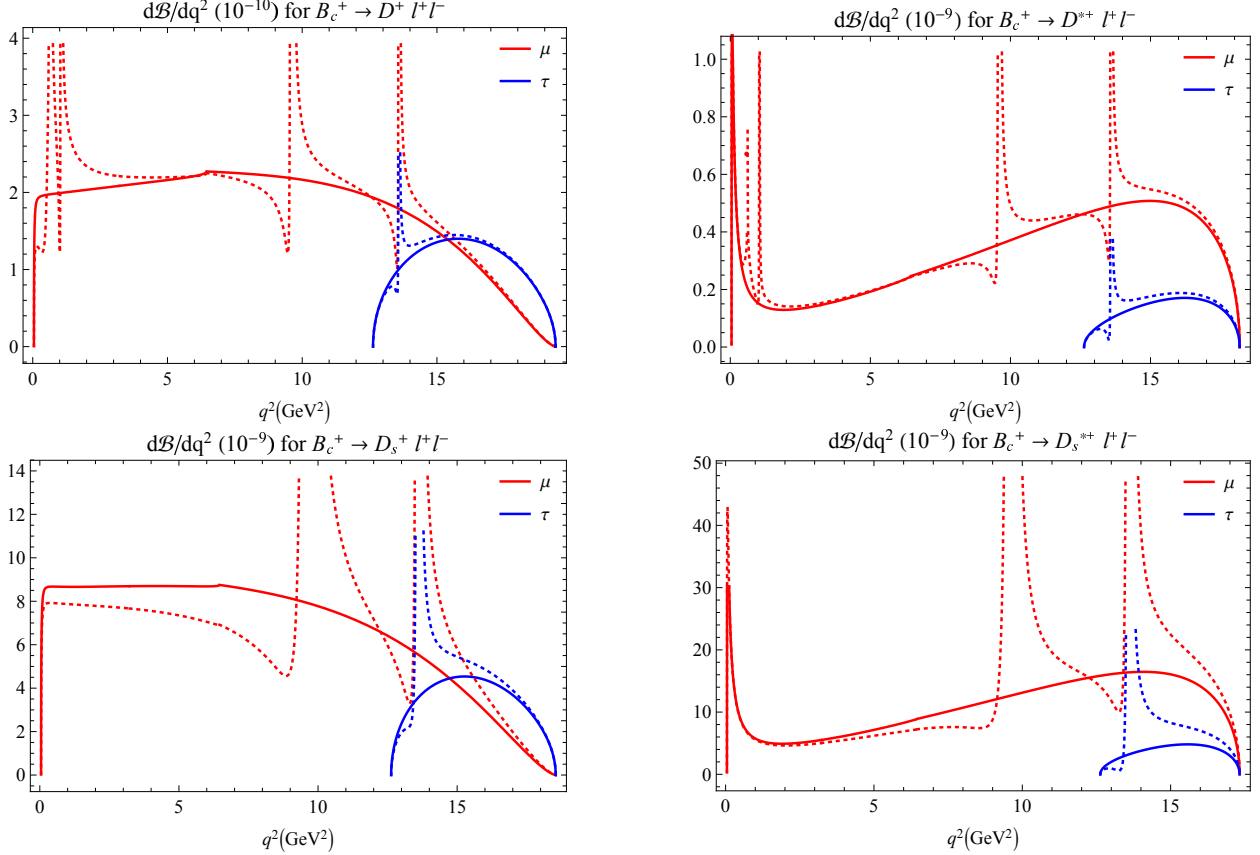


FIG. 6. Differential branching fraction

as well as in Ref. [107]. We also compare our results with theoretical predictions including different quark models, perturbative QCD and QCD sum rule approaches. Note that for the transitions corresponding to channels  $b \rightarrow sl^+\ell^-$ , we do not include the contribution coming from the light vector resonances because of the CKM suppression (of the order of  $\lambda^2$  in Wolfenstein representation); thus we neglect the effects of the second term in effective Hamiltonian Eq. (1). It is observed that our predictions for the non-resonant branching fractions for some channels are in good agreement with the other theoretical predictions. However, if we include the resonant contributions, our predictions are comparatively lower than the other theoretical approaches. In all the literature mentioned here, the contributions from the light vector resonances are not included for the transition corresponding to  $b \rightarrow dl^+\ell^-$ . Note that for the transition considered here, to the best of our knowledge and understanding, experimental data as well as lattice simulations results are not available and hence it is not logical to comment on the comparative credibility of the results from the theoretical approaches including current study.

TABLE IV. Branching fractions of  $B_c^+ \rightarrow D_{(s)}^{(*)+} \ell^+ \ell^-$  for  $\ell = e, \mu$  and  $\tau$ 

Channel	Non Resonance	Resonance	LFQM [41]	CQM [41]	pQCD [46]	RQM [48]
$10^9 \mathcal{B}(B_c^+ \rightarrow D^+ e^+ e^-)$	$3.430 \pm 0.359$	$2.640 \pm 0.210$	4.100	4.000	–	–
$10^9 \mathcal{B}(B_c^+ \rightarrow D^+ \mu^+ \mu^-)$	$3.422 \pm 0.358$	$2.634 \pm 0.210$	4.100	4.000	3.790	3.700
$10^9 \mathcal{B}(B_c^+ \rightarrow D^+ \tau^+ \tau^-)$	$0.729 \pm 0.118$	$0.502 \pm 0.085$	1.300	1.200	1.030	1.500
$10^8 \mathcal{B}(B_c^+ \rightarrow D^+ \nu^+ \nu^-)$	$1.375 \pm 0.136$	–	2.770	2.740	3.130	2.160
$10^9 \mathcal{B}(B_c^+ \rightarrow D_s^{*+} e^+ e^-)$	$7.001 \pm 0.506$	$4.960 \pm 0.251$	10.100	7.900	–	–
$10^9 \mathcal{B}(B_c^+ \rightarrow D_s^{*+} \mu^+ \mu^-)$	$5.916 \pm 0.341$	$3.882 \pm 0.160$	10.100	7.900	12.100	8.100
$10^9 \mathcal{B}(B_c^+ \rightarrow D_s^{*+} \tau^+ \tau^-)$	$0.717 \pm 0.035$	$0.518 \pm 0.025$	1.800	1.400	1.600	1.900
$10^8 \mathcal{B}(B_c^+ \rightarrow D_s^{*+} \nu^+ \nu^-)$	$2.566 \pm 0.119$	–	7.640	5.990	11.000	5.120
$10^7 \mathcal{B}(B_c^+ \rightarrow D_s^{*+} \gamma)$	$1.213 \pm 0.052$	–	–	–	–	–
$10^7 \mathcal{B}(B_c^+ \rightarrow D_s^+ e^+ e^-)$	$1.237 \pm 0.156$	$0.792 \pm 0.076$	1.360	1.330	–	–
$10^7 \mathcal{B}(B_c^+ \rightarrow D_s^+ \mu^+ \mu^-)$	$1.233 \pm 0.155$	$0.788 \pm 0.076$	1.360	1.330	1.560	1.160
$10^7 \mathcal{B}(B_c^+ \rightarrow D_s^+ \tau^+ \tau^-)$	$0.207 \pm 0.038$	$0.136 \pm 0.025$	0.340	0.370	0.380	0.330
$10^7 \mathcal{B}(B_c^+ \rightarrow D_s^+ \nu^+ \nu^-)$	$4.954 \pm 0.591$	–	9.200	9.200	0.129	6.500
$10^7 \mathcal{B}(B_c^+ \rightarrow D_s^{*+} e^+ e^-)$	$2.302 \pm 0.239$	$1.550 \pm 0.141$	4.090	2.810	–	–
$10^7 \mathcal{B}(B_c^+ \rightarrow D_s^{*+} \mu^+ \mu^-)$	$1.907 \pm 0.151$	$1.158 \pm 0.065$	4.090	2.810	4.400	2.120
$10^7 \mathcal{B}(B_c^+ \rightarrow D_s^{*+} \tau^+ \tau^-)$	$0.173 \pm 0.012$	$0.144 \pm 0.009$	0.510	0.410	0.520	0.350
$10^7 \mathcal{B}(B_c^+ \rightarrow D_s^{*+} \nu^+ \nu^-)$	$8.314 \pm 0.526$	–	31.200	21.200	40.400	13.500
$10^6 \mathcal{B}(B_c^+ \rightarrow D_s^{*+} \gamma)$	$4.412 \pm 0.254$	–	–	–	–	–

In order to explore the effects of leptons further in the final state, we study various observables such as forward backward asymmetry, longitudinal and transverse polarizations, and angular observables using the relations Eq. (33) and (35). These observables are plotted in the Fig. 7 - 9 and their expectation values in the whole  $q^2$  range are given in Tab. V. In these plots, we include the effects of both nonresonant and resonant contributions, where the peaks correspond to charmonia and light vector resonances. We also compute the expectation value of these observables in the different  $q^2$  bins corresponding to the

dropping the contributions from vector resonances. Very recently, Li Y. -L have studied the branching fractions and other observables for the channel  $B_c \rightarrow D_s^* \ell^+ \ell^-$  in the framework of covariant light front quark model (CLFQM) [91]. He computed the transition form factors using the modified Isgur-Wise function. We compare our results of the observables with CLFQM results in Tab. VI - VIII and it is observed that many of our results are not in agreement with the CLFQM results. The differences are mainly arising from the fact that the authors of [91] include the contribution of light vector resonances whereas we do not include light vector resonance for the transition corresponding to the quark channel  $b \rightarrow s \ell^+ \ell^-$ . Previously also the light vector resonances have been excluded for the transition corresponding to the quark channel  $b \rightarrow s \ell^+ \ell^-$  employing CCQM [86, 105]. To the best of our knowledge and understanding, these observables are yet to be studied using any other theoretical approaches and further these channels are also yet to be explored by the world wide experimental facilities. These observables are dependent on the lepton flavours and thus very important probe for the search of new physics beyond the standard model and therefore we may expect some light from the very recent run from the LHCb collaborations as well as from other  $B$  factories.

## V. SUMMARY AND CONCLUSION

In this article, we systematically study the rare semileptonic decay of  $B_c$  meson within the framework of covariant confined quark model. We have considered the channel  $B_c^+ \rightarrow D^{+(*)} \ell^+ \ell^-$  and  $B_c^+ \rightarrow D_s^{+(*)} \ell^+ \ell^-$  for all the lepton flavours. The necessary transition form factors are computed in the whole range of momentum transferred square and compared with the different theoretical approaches. Our results of the form factors are compatible with the other quark models. Using the form factors and Wilson coefficients, we have computed the rare semileptonic branching fractions and compared with other approaches. We also compute different other observables such as forward backward asymmetry, longitudinal and transverse polarizations, and angular observables. In present work, the computation of effective Wilson coefficients includes the contribution of charm resonances as well as the contribution of light vector resonances in the case of  $B_c^+ \rightarrow D^{+(*)} \ell^+ \ell^-$ . For  $B_c^+ \rightarrow D_s^{+(*)} \ell^+ \ell^-$ , we only include the contribution of vector charm resonances. It is observed that our predictions are systematically lower than those reported in literature and the main reason for the differences

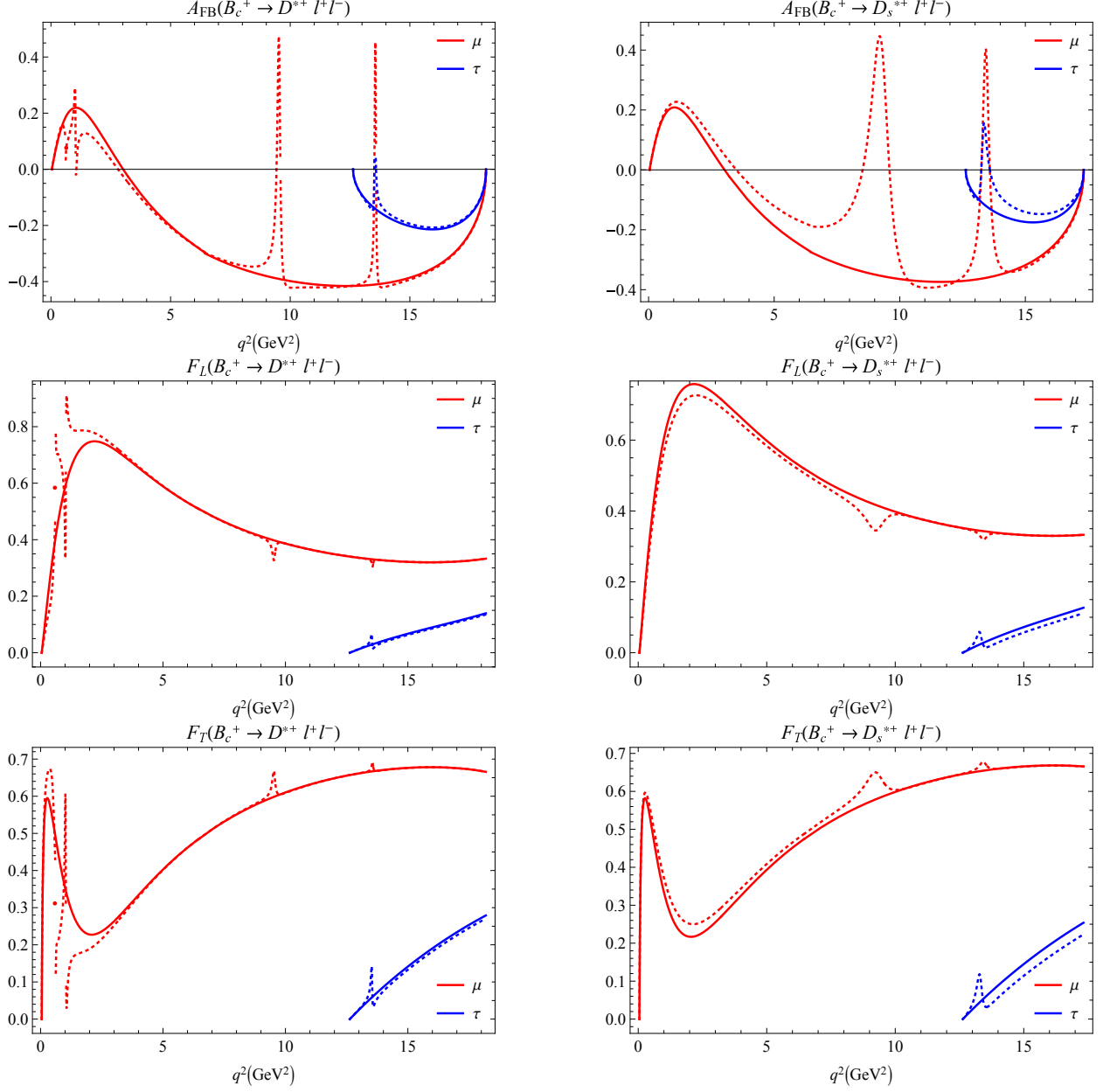


FIG. 7. Forward backward asymmetry, longitudinal and transverse polarizations (solid lines - excluding resonances, dashed lines - including vector resonances)

are attributed to the fact that we include the contribution of light vector resonances in the definition of effective Wilson coefficients as well as the choice of the numerical values of the Wilson coefficient.

To conclude, we have provided the complete description of rare semileptonic decays of  $B_c$  mesons in the framework of CCQM along with the different physical observables which would play an important role for the identification of these observables for future experimental

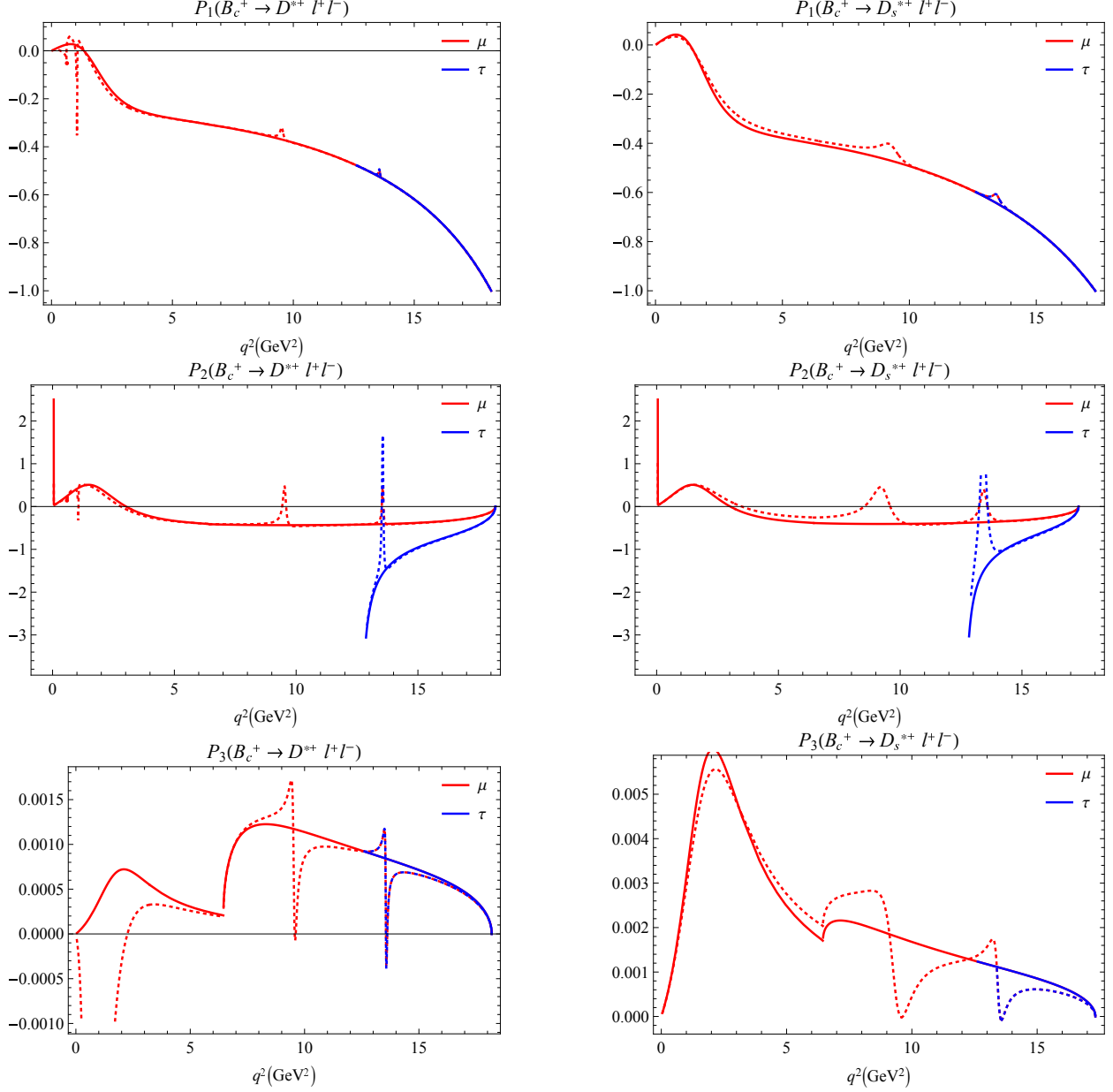


FIG. 8. Clean observables  $P_{1,2,3}$  in whole  $q^2$  range (solid lines - excluding resonances, dashed lines - including vector resonances)

facilities and also to look for the test of new physics beyond standard model, if any.

## ACKNOWLEDGEMENTS

NRS would like to thank INFN - Section of Naples for the Post-doctoral research grant.

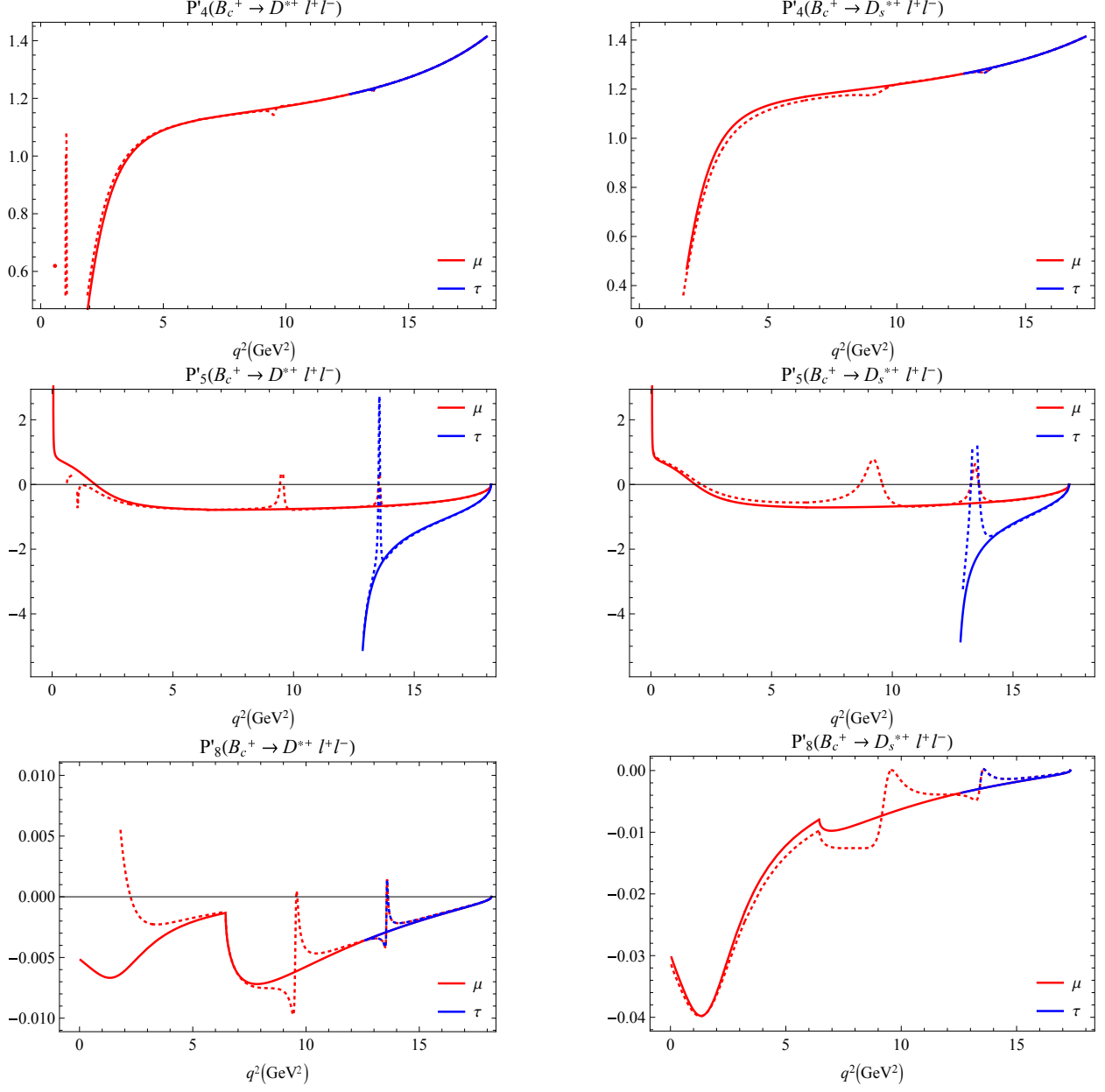


FIG. 9. Clean observables  $P_{4,5,8}$  in whole  $q^2$  range (solid lines - excluding resonances, dashed lines - including vector resonances)



TABLE V.  $q^2$ - averages of polarization observables over the whole allowed kinematic region for  $B_c^+ \rightarrow D^{*+}\ell^+\ell^-$  and  $B_c^+ \rightarrow D_s^{*+}\ell^+\ell^-$

Obs.	$B_c^+ \rightarrow D^{*+}\ell^+\ell^-$			$B_c^+ \rightarrow D_s^{*+}\ell^+\ell^-$		
	$e^+e^-$	$\mu^+\mu^-$	$\tau^+\tau^-$	$e^+e^-$	$\mu^+\mu^-$	$\tau^+\tau^-$
$-\langle A_{FB} \rangle$	0.186	0.239	0.188	0.131	0.178	0.134
$\langle F_L \rangle$	0.345	0.430	0.095	0.322	0.419	0.080
$\langle F_T \rangle$	0.634	0.536	0.200	0.655	0.544	0.163
$-\langle P_1 \rangle$	0.336	0.506	0.779	0.348	0.557	0.856
$-\langle P_2 \rangle$	0.195	0.297	0.627	0.134	0.218	0.548
$10^4 \times \langle P_3 \rangle$	2.176	2.298	4.801	9.085	14.211	4.754
$\langle P'_4 \rangle$	0.813	1.050	1.333	0.781	1.049	1.362
$-\langle P'_5 \rangle$	0.365	0.496	0.948	0.249	0.362	0.808
$10^2 \times \langle P'_8 \rangle$	2.257	2.436	-0.105	0.933	1.034	0.088
$-\langle S_3 \rangle$	0.107	0.136	0.078	0.114	0.152	0.070
$\langle S_4 \rangle$	0.190	0.252	0.092	0.179	0.250	0.078

TABLE VI. Angular observables in bins for the channel  $B_c^+ \rightarrow D^{*+}$ 

Obs.	bin	$e^+e^-$	$\mu^+\mu^-$	$\tau^+\tau^-$	Obs.	bin	$e^+e^-$	$\mu^+\mu^-$	$\tau^+\tau^-$
$\mathcal{B}$ $\times 10^9$	[1.1, 6.0]	$0.841 \pm 0.075$	$0.836 \pm 0.075$		$-\langle P_2 \rangle$	[1.1, 6.0]	0.184	0.187	
	[6.0, 8.0]	$0.518 \pm 0.031$	$0.516 \pm 0.031$			[6.0, 8.0]	0.410	0.411	
	[11.0, 12.5]	$0.679 \pm 0.032$	$0.677 \pm 0.302$			[11.0, 12.5]	0.433	0.434	
	[15.0,17.0]	$1.025 \pm 0.045$	$1.022 \pm 0.045$	$0.367 \pm 0.017$		[15.0,17.0]	0.346	0.347	0.745
$-\langle A_{FB} \rangle$	[1.1, 6.0]	0.087	0.087		$\langle P_3 \rangle$ $\times 10^4$	[1.1, 6.0]	-0.052	0.031	
	[6.0, 8.0]	0.316	0.315			[6.0, 8.0]	8.964	8.967	
	[11.0, 12.5]	0.420	0.420			[11.0, 12.5]	9.511	9.511	
	[15.0,17.0]	0.352	0.352	0.202		[15.0,17.0]	5.726	5.726	5.605
$\langle F_L \rangle$	[1.1, 6.0]	0.686	0.673		$\langle P_4' \rangle$	[1.1, 6.0]	0.877	0.881	
	[6.0, 8.0]	0.486	0.483			[6.0, 8.0]	1.131	1.132	
	[11.0, 12.5]	0.354	0.353			[11.0, 12.5]	1.199	1.199	
	[15.0,17.0]	0.321	0.321	0.086		[15.0,17.0]	1.306	1.306	1.310
$\langle F_T \rangle$	[1.1, 6.0]	0.314	0.310		$-\langle P_5' \rangle$	[1.1, 6.0]	0.571	0.576	
	[6.0, 8.0]	0.514	0.511			[6.0, 8.0]	0.769	0.772	
	[11.0, 12.5]	0.646	0.644			[11.0, 12.5]	0.730	0.731	
	[15.0,17.0]	0.679	0.677	0.181		[15.0,17.0]	0.532	0.533	1.143
$-\langle P_1 \rangle$	[1.1, 6.0]	0.243	0.244		$-\langle P_8' \rangle$ $\times 10^{-3}$	[1.1, 6.0]	-1.686	-1.584	
	[6.0, 8.0]	0.316	0.316			[6.0, 8.0]	5.380	5.381	
	[11.0, 12.5]	0.442	0.442			[11.0, 12.5]	4.071	4.071	
	[15.0,17.0]	0.706	0.706	0.717		[15.0,17.0]	1.366	1.366	1.309

TABLE VII. Angular observables in bins for the channel  $B_c^+ \rightarrow D_s^{*+}$ 

Obs.	bin	$e^+e^-$	[91]	$\mu^+\mu^-$	[91]	$\tau^+\tau^-$	[91]
$10^9 \times \mathcal{B}$	[1.1, 6.0]	$26.838 \pm 2.780$	6.240	$26.670 \pm 2.774$	6.220		
	[6.0, 8.0]	$14.864 \pm 1.112$	3.560	$14.787 \pm 1.109$	3.550		
	[11.0, 12.5]	$25.523 \pm 1.601$	2.830	$25.459 \pm 1.598$	2.830		
	[15.0,17.0]	$34.542 \pm 2.061$	2.560	$34.477 \pm 2.058$	2.560	$13.485 \pm 0.855$	0.980
$-\langle A_{FB} \rangle$	[1.1, 6.0]	0.002	0.061	0.003	0.061		
	[6.0, 8.0]	0.178	0.243	0.177	0.242		
	[11.0, 12.5]	0.385	0.340	0.384	0.339		
	[15.0,17.0]	0.270	0.254	0.270	0.254	0.138	0.143
$\langle F_L \rangle$	[1.1, 6.0]	0.651	0.815	0.640	0.817		
	[6.0, 8.0]	0.483	0.637	0.481	0.638		
	[11.0, 12.5]	0.366	0.446	0.365	0.446		
	[15.0,17.0]	0.331	0.352	0.330	0.352	0.079	0.410
$\langle F_T \rangle$	[1.1, 6.0]	0.349	0.185	0.344	0.183		
	[6.0, 8.0]	0.517	0.363	0.515	0.362		
	[11.0, 12.5]	0.634	0.554	0.632	0.554		
	[15.0,17.0]	0.669	0.648	0.667	0.648	0.159	0.590

TABLE VIII. Same as Tab. VII

Obs.	bin	$e^+e^-$	[91]	$\mu^+\mu^-$	[91]	$\tau^+\tau^-$	[91]
$-\langle P_1 \rangle$	[1.1, 6.0]	0.284	0.281	0.286	0.281		
	[6.0, 8.0]	0.401	0.408	0.401	0.408		
	[11.0, 12.5]	0.559	0.543	0.559	0.543		
	[15.0,17.0]	0.834	0.822	0.834	0.822	0.846	0.826
$-\langle P_2 \rangle$	[1.1, 6.0]	0.003	0.125	0.005	0.125		
	[6.0, 8.0]	0.229	0.446	0.230	0.446		
	[11.0, 12.5]	0.405	0.409	0.406	0.409		
	[15.0,17.0]	0.269	0.262	0.269	0.262	0.578	0.269
$10^4 \times \langle P_3 \rangle$	[1.1, 6.0]	35.914	1.840	35.835	1.840		
	[6.0, 8.0]	25.611	0.070	25.613	0.070		
	[11.0, 12.5]	12.148	24.210	12.148	24.210		
	[15.0,17.0]	5.165	34.420	5.165	34.420	4.993	20.080
$\langle P'_4 \rangle$	[1.1, 6.0]	0.883	0.908	0.887	0.898		
	[6.0, 8.0]	1.161	1.177	1.161	1.169		
	[11.0, 12.5]	1.247	1.240	1.247	1.236		
	[15.0,17.0]	1.354	1.350	1.354	1.347	1.358	0.561
$-\langle P'_5 \rangle$	[1.1, 6.0]	0.314	0.540	0.319	0.534		
	[6.0, 8.0]	0.505	0.766	0.507	0.761		
	[11.0, 12.5]	0.653	0.664	0.654	0.662		
	[15.0,17.0]	0.398	0.390	0.399	0.390	0.854	0.163
$-10^3 \times \langle P'_8 \rangle$	[1.1, 6.0]	22.141	1.196	22.033	1.164		
	[6.0, 8.0]	11.840	0.029	11.841	0.029		
	[11.0, 12.5]	3.873	7.054	3.873	7.030		
	[15.0,17.0]	0.977	6.147	0.977	6.137	0.928	1.467

- 
- [1] J. P. Lees *et al.* (BaBar), Phys. Rev. D **88**, 072012 (2013), arXiv:1303.0571 [hep-ex].
- [2] M. Huschle *et al.* (Belle), Phys. Rev. D **92**, 072014 (2015), arXiv:1507.03233 [hep-ex].
- [3] Y. Sato *et al.* (Belle), Phys. Rev. D **94**, 072007 (2016), arXiv:1607.07923 [hep-ex].
- [4] R. Aaij *et al.* (LHCb), Phys. Rev. Lett. **115**, 111803 (2015), [Erratum: Phys.Rev.Lett. 115, 159901 (2015)], arXiv:1506.08614 [hep-ex].
- [5] R. Aaij *et al.* (LHCb), Phys. Rev. Lett. **120**, 171802 (2018), arXiv:1708.08856 [hep-ex].
- [6] R. Aaij *et al.* (LHCb), Phys. Rev. Lett. **131**, 111802 (2023), arXiv:2302.02886 [hep-ex].
- [7] A. Mathad (LHCb), in *57th Rencontres de Moriond on Electroweak Interactions and Unified Theories* (2023) arXiv:2305.08133 [hep-ex].
- [8] R. Aaij *et al.* (LHCb), Phys. Rev. Lett. **120**, 121801 (2018), arXiv:1711.05623 [hep-ex].
- [9] J. Harrison, C. T. H. Davies, and A. Lytle (LATTICE-HPQCD), Phys. Rev. Lett. **125**, 222003 (2020), arXiv:2007.06956 [hep-lat].
- [10] A. Hayrapetyan *et al.* (CMS), (2024), arXiv:2401.07090 [hep-ex].
- [11] R. Aaij *et al.* (LHCb), Phys. Rev. Lett. **131**, 051803 (2023), arXiv:2212.09152 [hep-ex].
- [12] R. Aaij *et al.* (LHCb), Nature Phys. **18**, 277 (2022), [Addendum: Nature Phys. 19, (2023)], arXiv:2103.11769 [hep-ex].
- [13] R. Aaij *et al.* (LHCb), Phys. Rev. Lett. **128**, 191802 (2022), arXiv:2110.09501 [hep-ex].
- [14] S. Choudhury *et al.* (BELLE), JHEP **03**, 105 (2021), arXiv:1908.01848 [hep-ex].
- [15] R. Aaij *et al.* (LHCb), Phys. Rev. Lett. **125**, 011802 (2020), arXiv:2003.04831 [hep-ex].
- [16] R. Aaij *et al.* (LHCb), Phys. Rev. Lett. **122**, 191801 (2019), arXiv:1903.09252 [hep-ex].
- [17] R. Aaij *et al.* (LHCb), JHEP **08**, 055 (2017), arXiv:1705.05802 [hep-ex].
- [18] R. Aaij *et al.* (LHCb), JHEP **02**, 104 (2016), arXiv:1512.04442 [hep-ex].
- [19] R. Aaij *et al.* (LHCb), Phys. Rev. Lett. **113**, 151601 (2014), arXiv:1406.6482 [hep-ex].
- [20] R. Aaij *et al.* (LHCb), Phys. Rev. Lett. **111**, 191801 (2013), arXiv:1308.1707 [hep-ex].
- [21] J. P. Lees *et al.* (BaBar), Phys. Rev. D **86**, 032012 (2012), arXiv:1204.3933 [hep-ex].
- [22] N. Gubernari, D. van Dyk, and J. Virto, JHEP **02**, 088 (2021), arXiv:2011.09813 [hep-ph].
- [23] A. Khodjamirian, T. Mannel, A. A. Pivovarov, and Y. M. Wang, JHEP **09**, 089 (2010), arXiv:1006.4945 [hep-ph].
- [24] M. Bordone, G. Isidori, S. Mächler, and A. Tinari, (2024), arXiv:2401.18007 [hep-ph].

- [25] M. Algueró, A. Biswas, B. Capdevila, S. Descotes-Genon, J. Matias, and M. Novoa-Brunet, *Eur. Phys. J. C* **83**, 648 (2023), arXiv:2304.07330 [hep-ph].
- [26] N. Gubernari, M. Reboud, D. van Dyk, and J. Virto, *JHEP* **09**, 133 (2022), arXiv:2206.03797 [hep-ph].
- [27] T. Hurth, F. Mahmoudi, and S. Neshatpour, *Phys. Rev. D* **103**, 095020 (2021), arXiv:2012.12207 [hep-ph].
- [28] M. Ciuchini, A. M. Coutinho, M. Fedele, E. Franco, A. Paul, L. Silvestrini, and M. Valli, *Eur. Phys. J. C* **79**, 719 (2019), arXiv:1903.09632 [hep-ph].
- [29] M. Algueró, B. Capdevila, S. Descotes-Genon, P. Masjuan, and J. Matias, *Phys. Rev. D* **99**, 075017 (2019), arXiv:1809.08447 [hep-ph].
- [30] S. Descotes-Genon, L. Hofer, J. Matias, and J. Virto, *JHEP* **12**, 125 (2014), arXiv:1407.8526 [hep-ph].
- [31] A. Seuthe (LHCb), in *57th Rencontres de Moriond on QCD and High Energy Interactions* (2023) arXiv:2305.08216 [hep-ex].
- [32] R. Aaij *et al.* (LHCb), *Phys. Rev. D* **108**, 032002 (2023), arXiv:2212.09153 [hep-ex].
- [33] I. Adachi *et al.* (Belle-II, Belle), (2024), arXiv:2404.08133 [hep-ex].
- [34] R. Aaij *et al.* (LHCb), *JHEP* **04**, 029 (2017), arXiv:1701.08705 [hep-ex].
- [35] R. Aaij *et al.* (LHCb), *JHEP* **10**, 034 (2015), arXiv:1509.00414 [hep-ex].
- [36] R. Aaij *et al.* (LHCb Collaboration), *JHEP* **12**, 125 (2012), arXiv:1210.2645 [hep-ex].
- [37] R. Aaij *et al.* (LHCb Collaboration), *JHEP* **07**, 020 (2018), arXiv:1804.07167 [hep-ex].
- [38] M. Artuso, G. Isidori, and S. Stone, *New Physics in b Decays* (World Scientific, 2022).
- [39] D. London and J. Matias, *Ann. Rev. Nucl. Part. Sci.* **72**, 37 (2022), arXiv:2110.13270 [hep-ph].
- [40] R. Aaij *et al.* (LHCb), (2023), arXiv:2308.06162 [hep-ex].
- [41] C. Q. Geng, C.-W. Hwang, and C. C. Liu, *Phys. Rev. D* **65**, 094037 (2002), arXiv:hep-ph/0110376.
- [42] K. Azizi, F. Falahati, V. Bashiry, and S. M. Zebarjad, *Phys. Rev. D* **77**, 114024 (2008), arXiv:0806.0583 [hep-ph].
- [43] K. Azizi and R. Khosravi, *Phys. Rev. D* **78**, 036005 (2008), arXiv:0806.0590 [hep-ph].
- [44] A. Faessler, T. Gutsche, M. A. Ivanov, J. G. Korner, and V. E. Lyubovitskij, *Eur. Phys. J. direct* **4**, 18 (2002), arXiv:hep-ph/0205287.

- [45] H.-M. Choi, Phys. Rev. D **81**, 054003 (2010), arXiv:1001.3432 [hep-ph].
- [46] W.-F. Wang, X. Yu, C.-D. Lü, and Z.-J. Xiao, Phys. Rev. D **90**, 094018 (2014), arXiv:1401.0391 [hep-ph].
- [47] U. O. Yilmaz, Phys. Rev. D **85**, 115026 (2012), arXiv:1204.1261 [hep-ph].
- [48] D. Ebert, R. N. Faustov, and V. O. Galkin, Phys. Rev. D **82**, 034032 (2010), arXiv:1006.4231 [hep-ph].
- [49] P. Maji, S. Mahata, P. Nayek, S. Biswas, and S. Sahoo, Chin. Phys. C **44**, 073106 (2020), arXiv:2003.12272 [hep-ph].
- [50] P. Maji, S. Biswas, P. Nayek, and S. Sahoo, PTEP **2020**, 053B07 (2020), arXiv:2003.07041 [hep-ph].
- [51] R. Dutta, Phys. Rev. D **100**, 075025 (2019), arXiv:1906.02412 [hep-ph].
- [52] M. K. Mohapatra, N. Rajeev, and R. Dutta, Phys. Rev. D **105**, 115022 (2022), arXiv:2108.10106 [hep-ph].
- [53] M. Zaki, M. A. Paracha, and F. M. Bhutta, Nucl. Phys. B **992**, 116236 (2023), arXiv:2303.01145 [hep-ph].
- [54] J. N. Pandya, P. Santorelli, and N. R. Soni (2023) arXiv:2307.14245 [hep-ph].
- [55] N. R. Soni, A. Issadykov, A. N. Gadaria, Z. Tyulemissov, J. J. Patel, and J. N. Pandya, Eur. Phys. J. Plus **138**, 163 (2023), arXiv:2110.12740 [hep-ph].
- [56] N. R. Soni, A. Issadykov, A. N. Gadaria, J. J. Patel, and J. N. Pandya, Eur. Phys. J. A **58**, 39 (2022), arXiv:2008.07202 [hep-ph].
- [57] N. R. Soni, A. N. Gadaria, J. J. Patel, and J. N. Pandya, Phys. Rev. D **102**, 016013 (2020), arXiv:2001.10195 [hep-ph].
- [58] M. A. Ivanov, J. G. Körner, J. N. Pandya, P. Santorelli, N. R. Soni, and C.-T. Tran, Front. Phys. (Beijing) **14**, 64401 (2019), arXiv:1904.07740 [hep-ph].
- [59] N. R. Soni, M. A. Ivanov, J. G. Körner, J. N. Pandya, P. Santorelli, and C. T. Tran, Phys. Rev. D **98**, 114031 (2018), arXiv:1810.11907 [hep-ph].
- [60] N. R. Soni and J. N. Pandya, Phys. Rev. D **96**, 016017 (2017), [Erratum: Phys.Rev.D 99, 059901 (2019)], arXiv:1706.01190 [hep-ph].
- [61] R. L. Workman and Others (Particle Data Group), PTEP **2022**, 083C01 (2022).
- [62] S. Descotes-Genon, T. Hurth, J. Matias, and J. Virto, JHEP **05**, 137 (2013), arXiv:1303.5794 [hep-ph].

- [63] A. J. Buras and M. Munz, Phys. Rev. D **52**, 186 (1995), arXiv:hep-ph/9501281.
- [64] F. Kruger and L. Sehgal, Phys. Rev. D **55**, 2799 (1997), arXiv:hep-ph/9608361.
- [65] G. Buchalla, A. J. Buras, and M. E. Lautenbacher, Rev. Mod. Phys. **68**, 1125 (1996), arXiv:hep-ph/9512380.
- [66] N. Deshpande, J. Trampetic, and K. Panose, Phys. Rev. D **39**, 1461 (1989).
- [67] M. Jezabek and J. H. Kuhn, Nucl. Phys. B **320**, 20 (1989).
- [68] C. Lim, T. Morozumi, and A. Sanda, Phys. Lett. B **218**, 343 (1989).
- [69] M. Misiak, Nucl. Phys. B **393**, 23 (1993), [Erratum: Nucl.Phys.B 439, 461–465 (1995)].
- [70] P. J. O’Donnell and H. K. Tung, Phys. Rev. D **43**, 2067 (1991).
- [71] A. Ali, T. Mannel, and T. Morozumi, Phys. Lett. B **273**, 505 (1991).
- [72] C. Bobeth, M. Misiak, and J. Urban, Nucl. Phys. B **574**, 291 (2000), arXiv:hep-ph/9910220.
- [73] C.-H. Chen and C. Q. Geng, Phys. Rev. D **64**, 074001 (2001), arXiv:hep-ph/0106193.
- [74] W.-F. Wang and Z.-J. Xiao, Phys. Rev. D **86**, 114025 (2012), arXiv:1207.0265 [hep-ph].
- [75] M. Tanabashi *et al.* (Particle Data Group), Phys. Rev. D **98**, 030001 (2018).
- [76] G. V. Efimov and M. A. Ivanov, Int. J. Mod. Phys. A **4**, 2031 (1989).
- [77] G. V. Efimov and M. A. Ivanov, *The Quark confinement model of hadrons* (IOP, Bristol, 1993).
- [78] M. A. Ivanov and P. Santorelli, Phys. Lett. B **456**, 248 (1999), arXiv:hep-ph/9903446 [hep-ph].
- [79] T. Branz, A. Faessler, T. Gutsche, M. A. Ivanov, J. G. Korner, and V. E. Lyubovitskij, Phys. Rev. D **81**, 034010 (2010), arXiv:0912.3710 [hep-ph].
- [80] M. A. Ivanov, J. G. Korner, S. G. Kovalenko, P. Santorelli, and G. G. Saidullaeva, Phys. Rev. D **85**, 034004 (2012), arXiv:1112.3536 [hep-ph].
- [81] T. Gutsche, M. A. Ivanov, J. G. Korner, V. E. Lyubovitskij, and P. Santorelli, Phys. Rev. D **86**, 074013 (2012), arXiv:1207.7052 [hep-ph].
- [82] A. Salam, Nuovo Cim. **25**, 224 (1962).
- [83] S. Weinberg, Phys. Rev. **130**, 776 (1963).
- [84] M. A. Ivanov, J. G. Körner, and C. T. Tran, Phys. Rev. D **92**, 114022 (2015), arXiv:1508.02678 [hep-ph].
- [85] G. Ganbold, T. Gutsche, M. A. Ivanov, and V. E. Lyubovitskij, J. Phys. G **42**, 075002 (2015), arXiv:1410.3741 [hep-ph].



- [86] S. Dubnička, A. Z. Dubničková, A. Issadykov, M. A. Ivanov, A. Liptaj, and S. K. Sakhiyev, *Phys. Rev. D* **93**, 094022 (2016), arXiv:1602.07864 [hep-ph].
- [87] G. Buchalla and A. J. Buras, *Nucl. Phys. B* **548**, 309 (1999), arXiv:hep-ph/9901288.
- [88] M. Misiak and J. Urban, *Phys. Lett. B* **451**, 161 (1999), arXiv:hep-ph/9901278.
- [89] J. Brod, M. Gorbahn, and E. Stamou, *Phys. Rev. D* **83**, 034030 (2011), arXiv:1009.0947 [hep-ph].
- [90] A. Issadykov and M. A. Ivanov, *Mod. Phys. Lett. A* **38**, 2350006 (2023), arXiv:2211.10683 [hep-ph].
- [91] Y.-S. Li and X. Liu, *Phys. Rev. D* **108**, 093005 (2023), arXiv:2309.08191 [hep-ph].
- [92] R. Aaij *et al.* (LHCb Collaboration), *JHEP* **02**, 104 (2016), arXiv:1512.04442 [hep-ex].
- [93] S. Wehle *et al.* (Belle Collaboration), *Phys. Rev. Lett.* **118**, 111801 (2017), arXiv:1612.05014 [hep-ex].
- [94] R. Aaij *et al.* (LHCb), *JHEP* **09**, 179 (2015), arXiv:1506.08777 [hep-ex].
- [95] R. Aaij *et al.* (LHCb), *JHEP* **09**, 146 (2018), arXiv:1808.00264 [hep-ex].
- [96] A. Arbey, T. Hurth, F. Mahmoudi, D. Martínez Santos, and S. Neshatpour, *Phys. Rev. D* **100**, 015045 (2019), arXiv:1904.08399 [hep-ph].
- [97] K. Kowalska, D. Kumar, and E. M. Sessolo, *Eur. Phys. J. C* **79**, 840 (2019), arXiv:1903.10932 [hep-ph].
- [98] A. K. Alok, A. Dighe, S. Gangal, and D. Kumar, *JHEP* **06**, 089 (2019), arXiv:1903.09617 [hep-ph].
- [99] G. Hiller and M. Schmaltz, *Phys. Rev. D* **90**, 054014 (2014), arXiv:1408.1627 [hep-ph].
- [100] G. Hiller, D. Loose, Nis, and I. Zic, *Phys. Rev. D* **97**, 075004 (2018), arXiv:1801.09399 [hep-ph].
- [101] A. Crivellin, D. Müller, and T. Ota, *JHEP* **09**, 040 (2017), arXiv:1703.09226 [hep-ph].
- [102] P. Ko, Y. Omura, Y. Shigekami, and C. Yu, *Phys. Rev. D* **95**, 115040 (2017), arXiv:1702.08666 [hep-ph].
- [103] B. Kindra and N. Mahajan, *Phys. Rev. D* **98**, 094012 (2018), arXiv:1803.05876 [hep-ph].
- [104] J. Matias, *Phys. Rev. D* **86**, 094024 (2012), arXiv:1209.1525 [hep-ph].
- [105] S. Dubnička, A. Z. Dubničková, N. Habył, M. A. Ivanov, A. Liptaj, and G. S. Nurbakova, *Few Body Syst.* **57**, 121 (2016), arXiv:1511.04887 [hep-ph].
- [106] M. Wirbel, B. Stech, and M. Bauer, *Z. Phys. C* **29**, 637 (1985).

- [107] T. Blake, G. Lanfranchi, and D. M. Straub, *Prog. Part. Nucl. Phys.* **92**, 50 (2017), arXiv:1606.00916 [hep-ph].